Oluwatobi Olobayo[1, 2*], Mads Huuse[2], & Christopher AL Jackson[3]

[1] *Data, Digital and Technology Limited, Bartle House, 9 Oxford Court, Manchester, M2 3WQ, UK (tobi@ddatconsulting.com)*

[2] *The University of Manchester, Manchester M13 9 PL, UK (mads.huuse@manchester.ac.uk)*

[3] *Jacobs, Manchester, UK (c.jackson@imperial.ac.uk)*

This manuscript has been submitted to Marine and Petroleum Geology but has not undergone peer review. Subsequent versions of this manuscript may have slightly different content. If accepted, the final version of the manuscript will be made available via 'Peer reviewed Publication DOI' link on the right hand side of this webpage. Please feel free to contact any of the authors; we welcome your feedback.

Regionally Developed Giant Sand Injection Complexes in the Northern North Sea

Oluwatobi Olobayo[1, 2*], Mads Huuse[2], & Christopher AL Jackson[3]

[1] *Data, Digital and Technology Limited, Bartle House, 9 Oxford Court, Manchester, M2 3WQ, UK*

[2] *The University of Manchester, Manchester M13 9 PL, UK*

[3] *Jacobs, Manchester, UK*

**Correspondence (tobi@ddatconsulting.com)*

Abstract

The Northern North Sea (NNS) is an archetype Giant Injected Sand Province (GISP). Previous studies have documented individual stratigraphically-bound injectite complexes in the North Sea and beyond. Despite two decades of continuous studies, there are still speculations in terms of parent sand identification, visible pathways, fluid source, overpressure generation mechanisms and triggers. This study is based on a 29,000 km^2, 3D seismic volume calibrated to boreholes, and documents for the first time, the stratigraphy of the NNS Basin GISP, spanning five (5) injection episodes over 80 m.y. Sizes range from 500 m to 8 km wide and from 50 to 250 m in height, for individual intrusions. Well data confirms sandstones lithology emplaced within polygonally-faulted mudstones. Fluid budget has been attributed to a combination of several sources, which includes hydrocarbons and diagenetically-released water from opal A to opal CT transformation, smectite to illite transformation and physical compaction of sediments. Basin modelling in the North Viking Graben shows that hydrocarbon generation started during Late Cretaceous for oil and Late Neogene for gas. Presence of sandstone injectites suggests breach in the sealing host rocks, therefore needs to be incorporated into existing stratigraphic framework for accurate reservoir models in basins where they have been encountered.

1.Introduction

Sandstone injectites have been described as far back as the early 1900's (Jenkins 1930), however their petroleum significance was only realized in the last two decades with the help of high-resolution, 3D seismic data integrated with well log and outcrop analogues. Data integration has improved identification, detailed interpretation and implications within sedimentary basins such as North Sea basin, Faroe-Shetland basin and San Joaquin valley where Large Scale Intrusion Provinces (LSIPs) have been documented in detail (Cartwright 2010). Recognition range from cores , to wireline (Duranti & Hurst 2004) to outcrop (Thompson

et al. 2007; Hurst et al. 2011, 2016) to seismic scale (Huuse & Mickelson 2004;; Jackson 2007; Lonergan et al. 2000; Schwab et al., 2014).

The study area is located in the North Viking Graben and falls within the North Sea Sand Injectite Province (NSIP) (Fig. 1a). Previous studies have focused on individual sand injectite complex or multiple sand injectites within one or two stratigraphic interval, but this study presents the first-ever documentation of a regional detailed study in the North Viking Graben that ties everything together in time and space from upper Cretaceous to Pliocene units allowing consideration of possible parent bodies, fluid sources and multiple timing of emplacement for the injectites. The study is also very unique, as it gives insight on both small-scale injectites (core-scale) and larger bodies that extend for hundreds of metres to kilometre, similar to those observed in seismic data. 29,000 km^2 of 3D seismic MegaSurvey (courtesy of PGS), 38,000 km long 2D seismic profiles (TGSNOPEC), and wireline logs from over 50 wells were made available for the study. Completion logs, biostratigraphic data and well reports were also available from the Norwegian Petroleum Directorate (NPD.NO) website.

Additional geological features observed within the studied interval include polygonal fault networks and silica diagenetic transformation zones (Opal A - CT and CT - Quartz silica phases), both formed as a result of contraction and de-watering of fine-grained lithology, usually mudstones during shallow burial (Lonergan et al. 2000; Bureau et al. 2013). Evidence of silica diagenetic transformation within Paleocene to Oligocene sediments in the study area was first documented by Rundberg (1991) and during diagenesis, sediments are greatly compacted leading to dramatic porosity reduction, release of significant volume of water and generation of excessive overpressure within sediments (Davies et al. 2006).

The main aim of this study is to (1) document the occurrence, geometry and distribution of sand injectites (2) investigate their relationship with polygonal faults or underlying Mesozoic faults (3) identify potential parent sand bodies in the area (4) investigate the timing of emplacement of sand injectites and (5) discuss possible priming and triggering mechanisms associated with their formation.

2. Regional Setting

The Cenozoic North Sea basin formed as a thermal sag basin above pre-existing, rift-related structures, associated with extensional events during the last two phases of the rifting in the Permo-Triassic, and the Late Jurassic-to-Early Cretaceous (Ziegler 1990). Sediment thickness is greatest in the North Viking and Sogn Grabens reaching up to 5s two-way-time (TWT) (Ahmadi et al. 2003). The study area is located between 60-62º latitude and 1-5º longitude. It is bounded by the Norwegian coastline to the east, the Shetland Isles to the west, North Atlantic in the north and to the south by the South Viking Graben (Fig. 1). The study interval encompasses the Cenozoic and Cretaceous interval, bounded above and below by present-day seabed and base Cretaceous unconformity, respectively (Fig. 2). Sediments are dominantly fine-grained mudstones with large, sand-rich fans and channel systems, which are deposited during uplifts along the basin margins (Martinsen et al. 1999; Jordt et al. 2000; Ahmadi et al. 2003; Rundberg & Eidvin 2005). Sandstones were

sourced from both the east (Norway) and the west (Shetlands) (Jordt et al. 2000; Ahmadi et al. 2003; Goledowski et al. 2012; Olobayo et al. 2015 PhD thesis).

The stratigraphic evolution of the Cenozoic North Sea basin is controlled mainly by tectonics, eustatic and climatic processes; however, post-depositional processes, such as sub-surface remobilization and injection of sands, polygonal faulting and diagenetic transformation have greatly contributed to the present-day configuration of the basin (Huuse & Mickelson 2004; Davies et al. 2006; Løseth et al. 2013).

The Cretaceous stratigraphy is divided into Cromer Knoll and Shetland groups, composed mainly of thick mudstones throughout the study area (Fig. 2a), but very thin or almost absent over the Troll fault blocks. Large slope fan, channels and terminal fans, belonging to the Kyrre Formation in the Upper Cretaceous, were mapped along the Maløy slope (Jackson et al. 2011). The overlying Cenozoic interval is divided into three main groups: Rogaland, Hordaland and Nordland Groups. Uplifts along the basin margins, related to break-up of North Atlantic, resulted in deposition of clastic sediments from main areas, such as the Shetland platform and western Norway (Ahmadi et al. 2003). During the Late Paleocene to Early Eocene, separation of Norway and Greenland resulted in volcanic activity that deposited ash-rich, tuffaceous deposits, which formed the Balder Formation (Jordt et al. 2000; Ahmadi et al. 2003). This marks the uppermost part of the Rogaland group; a regional marker horizon across the North Sea. Uplifts along the basin margins resulted in deposition of channel-lobe and sand-rich fans into the basin (Huuse & Mickelson 2004). The Hordaland Group comprises of siliciclastic sediments, bounded above and below by the mid-Miocene unconformity and the uppermost Balder Formation, respectively (Fig. 2). Deposition within the basin at this time was characterized by fine-grained, smectite-rich mudstones and coarser-grained, siliceous-rich mudstones in the Eocene and Oligocene intervals, respectively (Rundberg 1991, Thyberg et al. 2010). The Eocene-Oligocene transition records significant events globally; these include: changes from greenhouse to icehouse conditions, reduction in water bottom temperature, global mass extinction, faunal and mineralogical changes from smectite-rich to biogenic, and deposition of silica-rich sediments (Rundberg 1991; Rundberg & Eidvin 2005).

The mid-Miocene unconformity (MMU) represents a period of significant erosion in the North Sea and separates the Hordaland from the Nordland Group with a time-gap of about 15 m.y (Fig. 2) (Isaksen & Tonstad 1989; Martinsen et al. 1999; Rundberg & Eidvin 2005; Løseth et al. 2013). It is occasionally mounded in the study area, due to effect of underlying units (Olobayo et al. 2015 PhD thesis). The Utsira Formation (Late Miocene or Early Pliocene) is dominated by sandstone and bounded at the base by the MMU or base Miocene surface. The Utsira Formation is overlain by westwardly-prograding, Pliocene-age clastic wedge, clinoforms that are truncated at their tops by the regional Pleistocene unconformity, these are sourced from the Norwegian mainland (Jordt et al. 2000).

The North Sea is one of the most prolific basins in the world with an active petroleum system since the Mesozoic, which continues till the Cenozoic in the North Viking Graben; with the Late Jurassic Kimmeridge Clay Formation (Kubala et al. 2003) as the main source rock. Hydrocarbon exploration and production activities in the Northern North Sea (NNS) was concentrated in the Mesozoic succession with giant fields such as Troll, Statfjord, Snorre and Gullfaks. However, in the last few years, there has been increasing interest in the overlying, Tertiary intervals. Hundreds of wells drilled to target Mesozoic accumulations that

penetrated some of the Cenozoic sandstones have recorded mostly only traces of hydrocarbon or completely water-wet with exception of the Peon and Gullfaks (34/10-8-A) discoveries within the Pleistocene and Paleocene intervals respectively. Sand injectites constitute great reservoirs or enhanced reservoir connectivity in adjacent parts of the study area such as the Outer Moray Firth and South Viking Graben but not the case in the NNS (Fig. 1a).

3. Characteristics and distribution of amplitude anomalies in the Northern North Sea

Discordant reflections emanating from steep-sided mounds and other style of anomalies may be either high, or low amplitude, positive or negative reflection (Tab.1). The seismic response is dependent on a number of factors, such as porosity, cementation, pore fluid, sandstone thickness, continuity, acoustic properties of both the sand and the encasing mudstones, geometrical complexity, seismic wave propagation and energy attenuation (Huuse et al. 2004, 2007, 2010; Hurst et al. 2011).

Following the Cenezoic classification mapping carried out by Jordt et al. 2000, 10 sequences have been mapped in the study area, CSS0 – CSS9 bounded at the base of CSS0 by the Base Cretaceous Unconformity and top of CSS9 by the present day seabed (Figs. 2 & 3). For ease of description and simplicity, anomalies described in this study are discussed based on the CSS unit they are located in. The anomalies have only been observed in CSS0 – CSS2, CSS4, CSS6 and CSS7, but not in CSS3, CSS5, and CSS8 – CSS9 (Tab. 1), hence the following section of observations will be based only on the units with anomalies. Details on their geometries, dimensions, spatial distribution, and relationship with background stratigraphy, timing of emplacement and potential parent bodies are discussed using individual case studies from the area.

CSS0-emplaced anomalies – A prominent Upper Cretaceous fan was mapped within the CSS0 sequence by Jackson (2007). Random seismic profiles along the depositional features within the unit reveal high-amplitude, bedding concordant anomalies, labelled **'c'**, emplaced within low-amplitude background stratigraphy in Turonian interval of CSS0 (Fig. 4). Strata terminations, such as erosional truncations, are observed below them. A series of high-amplitude, discordant anomalies, labelled **'d'**, inform of wings on the seismic profiles, are identified coming upwards from the sides of the concordant anomalies **'c'** (Figs. 4e – g). The discordant parts crosscut some 7 - 90 ms TWT of the host stratigraphy and average measured dip angle is 7º. Although jack-ups are rarely preserved above anomalies, thinning of overburden was observed in the northern anomaly (Fig. 7d). These anomalies are restricted to the northeasterly part of the area, the Maløy slope (Fig. 3a) and have also been extensively mapped by Jackson (2007).

CSS1-emplaced anomalies – High-amplitude anomalies are also observed within CSS1 (Figs. 2, 3 & 5). Two main styles of anomalies, observed within the CSS1 unit, include: high-amplitude, V or U-shaped, discordant anomalies and mound-shaped anomalies (Fig. 5). The first style of anomalies, identified in this interval, is characterized by highly discordant reflections, with individual flank dips, ranging between 17° and 32° (Table 1). They are typically V or U-shaped in seismic cross-sections and crosscut about 90 to 210 metres of background strata. Upper width measurements of these anomalies range between 440 and 1290 m. In 3D, they exhibit conical and saucer-shape geometry and make up about 99% of the total anomalies within the unit. The unit which anomalies are emplaced are often offset by polygonal faults. The majority of the

amplitude anomalies have a common datum, which is often folded or jacked up locally, where anomalies are observed (Fig. 5c). The second style of anomaly, mound-shaped observed within CSS1 unit is characterized by mounds, with onlaps on the outer layer and a relatively flat base (Fig. 5). Only one single mound was observed within the unit and thickness map shows it is about 40m thick. Below the mound are series of high-amplitude, discordant reflections that most likely belongs to the V or U-shaped anomalies described in the first style of anomalies above (Fig. 5c). Anomalies within CSS1 are restricted to the northeastern part of the study area and form a NE-SW trend, similar to orientation of the underlying structural highs and faults (Fig. 3b). The distribution of the anomalies does not closely match the eastern depocenter but rather they extend away from the it towards the basin centre. Spatial relationship suggests that the underlying structural highs may have influenced distribution of the anomalies.

CSS2-emplaced anomalies – The CSS2 is bounded above and below by the Eocene - Oligocene unconformity (H3) and uppermost Balder surface (H2) (Fig. 2). Main depocentres in the CSS2 occur along the margins with thickness reaching up to 450 ms (490 m) (Fig. 3c). The most striking features observed in seismic data within this unit are high-amplitude, crosscutting anomalies (Fig. 6). They are usually V, U, W-shaped in cross section with well-defined 3D geometries and oval-shaped in plan view (Fig. 6d). Although, they can also form very complex geometries outside the common ones mentioned above, thus making detailed mapping difficult. They crosscut about 120 – 215 m of the Eocene strata with their apexes either directly above the uppermost Balder surface or about 100 m above it. Average dip angle measured is about 25º similar to those described in Eocene section in other parts of the North Sea (Table 1). Amplitude extraction above the uppermost Balder reveals patches of high-amplitudes representing the distribution of anomalies (Fig. 6g). These anomalies are concentrated in the western part of the study area (Fig. 3c). 3D image of the conical anomalies above the uppermost Balder surface shows relationship with underlying structural highs associated with Mesozoic hydrocarbon fields such as the Gullfaks (Fig. 6f). This observation is consistent with previous work done in the Tampen Spur area (Huuse & Mickelson 2004). Upward bending of the uppermost Balder surface and slight distortion of the seismic data is observed below individual intrusions (Figs. 6a - c). Upward bending of the surface is usually formed from presence of a formation with a much higher velocity than surrounding lithology, thereby creating pull-up in the stratigraphy below the higher velocity lithology (Huuse *et al.* 2004; Andresen *et al.* 2009; Monnier *et al.* 2014). In some cases, the distortion can be traced as far as into the Cretaceous interval. Forced fold or jack up (20 – 30 m high) of the Eocene-Oligocene unconformity is observed above the anomalies with Early Oligocene-aged sediments onlapping onto the forced folds.

Sandstones in the Eocene (CSS2) have not been deliberately targeted by exploration wells in the area; however few wells intersected the high-amplitude anomalies and confirmed presence of sandstone lithology (Figs. 6a – c). Wells 34/10-30 encountered 40 m and 50 m of sandstone units at about 1400 metres and 1600 m respectively within the Horda Formation mudstones. Well 34/10-2 encountered 4 sandstone packages with thickness range from 15 to 30 m. The lowest sandstone packages encountered by these wells are calibrated to the discordant margins of the amplitude anomalies within the CSS2. Discordant anomalies intersected by wellbores above the Snorre Field in block 34/7 also confirm presence of tens of metres of sands (Huuse & Mickelson 2004).

CSS4-emplaced anomalies – The CSS4 unit is bounded below by Eocene-Oligocene unconformity (H3) and above by base Miocene surface (H6) in the basin centre and western part, but by the mid-Miocene unconformity (MMU) in the northern and eastern part of the basin (Fig. 2). Main depocentre is along the western margin close to the Shetlands, where thickness reaches up to 1100 m (Fig. 3d). The unit encompasses the entire Oligocene succession and pervasively deformed by polygonal faults (Figs. 7 & 8). The most conspicuous features observed within the CSS4 unit are series of high-amplitude, discordant anomalies that cross cuts polygonally faulted mudstone succession (Figs. 7 & 8). They form wide range of geometries; from simple, isolated conical and saucer-shape to very complex clusters of V or W shape. Average dip angle is 20º and height range between 60 to 215 m (Table 1). The complex anomalies also tend to be wider with some extending up to 8 km and could have formed from amalgamation of single conical-shaped ones.

Discordant margins of these anomalies sometimes follow polygonally-fractured networks when preferentially oriented but also cross cuts the fault networks (Fig. 7). Spatial relationship exists between forced folding of the overlying MMU and the location of discordant amplitude anomalies with the unit. Folding or jack up is more pronounced above the complex anomalies than the simple conical-shaped ones, this is observed from measuring the height of the fold/jack up above the anomalies from the mid-Miocene unconformity. Values range from < 5 ms to 90 ms for the simple-shaped to complex anomalies respectively. These forced folds or jack up created above anomalies within CSS4 are more pronounced than those in the underlying intervals.

Several examples of the saucer-shaped anomalies encountered within CSS4 exhibit prominent uplift or jack up of the basal or concordant part labelled **'s'** (sill) (Fig. 8). Jack up height, which is the thickness between the present location of the concordant part and the location before the jack up is within the range of 30 to 90 m. Reflections are primarily low and chaotic locally below the jack up part. Figure 8 shows a 2 km long basal sill flanked on both sides by discordant margins '**w**' known as wings or dykes. In cross section, the margins crosscut some 100–150 ms (120-160 m) of the Oligocene unit and transforms into a bedding concordant unit/sill at the top of the wing, which extends about 50 m away from the margins. The sill corresponds to a boundary that separates underlying medium-amplitude, parallel and continuous reflections from an upper unit, characterized by low-amplitude, parallel and continuous reflections (green dotted horizon; Fig. 8b). The configuration is very similar to the Volund structure with the conformable event coinciding with Early Eocene horizon (Top Frigg) interpreted as an unconformity or a paleo-seabed (Huuse *et al.* 2004). About 50 ms above the saucer-shaped anomaly, a mounded-shaped feature is observed in cross section. It is 80 m high, flank angle >10°, about 2.5 km in diameter and located on top of the MMU (Fig. 8). A small depression labelled '**p**', characterized by a negative topography is observed at the base of the mound on the mid-Miocene unconformity. Although embedded within upper CSS6 unit, mound emplacement is considered to be related to underlying saucer-shaped anomaly in CSS4 unit.

Discordant anomalies, described in CSS4, primarily lie above a high-amplitude, crosscutting positive reflection (Opal C-CT in Fig. 7). The reflection, which is characterized as a strong trough, is indicative of an increase in acoustic impedance on seismic data, created by a downward increase in density and sonic log, and interpreted as Opal A – CT silica diagenetic boundary (Rundberg 1991; Thyberg *et al.* 2010; Wrona *et al.* 2015). The boundary formed from conversion of sediment rich in amorphous, biogenic silica (Opal – A) to a more stable, crystalline silica Opal – CT through the process of dissolution and precipitation (Rundberg

1991). Relationship between discordant anomalies and diagenetic boundary was first observed in the Faroe-Shetland basin, North Sakhalin, Santa Cruz (Davies *et al.* 2006, Thompson *et al.* 2007).

Some of the amplitude anomalies within CSS4 were penetrated by exploration wells. Well 35/8-2 intersected the discordant wing of saucer-shaped anomaly and encountered a 24 m thick sandstone encased in Horda Fm mudstones (Fig. 7). Also in block 34/10, wells that penetrated high amplitude anomalies confirmed presence of thick sandstone units (Davies *et al.* 2006). Petrophysical log analysis revealed excellent reservoir properties in the sandstone with porosity as high as 32% and a net-to-gross of 80% (In-house analysis). The sandstone is however, brine filled. Saucer-shaped anomaly in figure 8 is not intersected by any well, making lithology of anomalies in the unit difficult to constrain but based on similar seismic amplitude responses with underlying Eocene fan and lithological calibration from similar features in the area, we infer that these anomalies are conical and saucer-shaped sandstone intrusions sandstone. It is also not possible to determine the lithology of the mound, due to lack of well penetration. However, lithology is assumed to be sandstone based on the following observations: (i) top surface represented by an increase in acoustic impedance, (ii) location above the saucer-shaped anomaly interpreted as sandstone intrusion, (iii) gentle draping of overlying prograding sediments suggesting differential compaction, (iv) lack of any evidence of salt, carbonate or igneous materials in the area and (v) strong similarity in size and shape to the giant sand mound/sand extradite, described in the Norwegian-Danish Basin (Andresen *et al.* 2009).

CSS6-emplaced anomalies – The CSS6 is bounded above and below by the base Pliocene unconformity (H8) and mid-Miocene unconformity (H7), respectively (Fig. 2). The main depocentres in the CSS6 are located in the northeasterly and southwesterly parts of the basin (Fig. 3). Thickness and character of this unit is variable across the basin and very dependent on the morphology of the mid-Miocene unconformity (Fig. 9). The MMU, which is the top of the Hordaland group, represents a high-amplitude trough reflection, mappable across the North Sea. While some workers believed the unconformity was formed as a result of sub-aerial exposure and erosion (Martinsen *et al.* 1999), others proposed a sub-marine erosional formation (Rundberg & Eidvin 2005). The morphology of the surface is either parallel to surrounding erosional reflections, or irregularly mounded, due to jack-up created by underlying high-amplitude, discordant anomalies. No polygonal faults are observed from this unit.

Two different types of mounds are recognized within CSS6 in the study area: (i) those formed from forced folds above underlying high-amplitude, discordant anomalies and (ii) those formed due to present of sediments within the unit (Fig. 9). The example presented here is irregularly shaped, elongate mound complex, located in the eastern part of the area, within quadrant 35. This example shows distinctively the two types of mounds in the CSS6 unit (Fig. 9). The mound complex presented here and similar ones have been previously studied by Løseth *et al.* (2013). The mound complex is about 5 km wide, 12 km long and up to 150 m high (Fig. 9). The unit thins considerably above intervals with high-amplitude, discordant anomalies and represented in cool colours from the TWT thickness map of the interval. In plan view, the thin units have circular to oval-shape geometry and are located in between thicker units. At discrete locations where the second type of mounds is thinnest, it coincides with thicker underlying CSS4 units and vice versa.

Generally, the CSS6 unit in the study area encompasses the Utsira Formation, which is mainly dominated by thick sandstone units of the Utsira member (Fig. 9). Sandstone thickness varies considerably within the unit across the entire study area (Isaksen & Tonstad 1989). For example well 35/11-12 penetrated up to 100 metres of sandstones, but well 35/8-4 encountered only very thin sandstone beds. No cores are available from these wells, but gamma ray logs reveal blocky log patterns. Volume of sandstone estimated within the mound complex presented above is about 240 km^2.

CSS7-emplaced anomalies – CSS7 unit is bounded above and below by the base Pleistocene and base Pliocene surfaces, respectively (Fig. 2). The interval encompasses the Pliocene-aged, westwardly prograding clinoforms which downlaps onto underlying sediments of Early Pliocene or Late Miocene age. Depocentre is greatest in the northwesterly part of the study area, where thickness reaches up to 1000 ms TWT.

At approximately 50–80 ms above the mid-Miocene unconformity, a mound-shaped, amplitude anomaly is observed with the CSS7 unit (Fig. 10) (Huuse & Mickelson 2004; Løseth *et al.* 2013). The surface, bounding the top of the mound complex, is characterized by a high-amplitude, trough reflection, which locally is slightly mounded, while the lower bounding surface is relatively flat and conformable with surrounding. Thickness between the two reflections represents the thickness of the mound complex. This thickness is variable across the mound complex and significantly controlled by forced folds/jack ups created by underlying anomalies. Thickness reduces considerably above folds or completely absent. Only one mound complex is recognized within CSS7 unit and restricted to quadrant 34 above the Snorre Field.

Wells in block 34/7 and 34/4 penetrated thick sandstone units within the mounded unit. Sand thickness decreases gradually away from the centre. Well 34/7-4 encountered about 80 metres of sandstones and well 34/4-7, which is less than 2 kilometres away, penetrated only about 33 metres (Fig. 10). Gamma ray log often show two sandstone packages separated by thin mudstone bed. Sidewall cores examined from the upper package in well 34/4-7 reveal fine-grained, rounded to sub-rounded sands (Løseth *et al.* 2013). Sandstone units are very thin or completely absent above forced folds. Seismic profile shows anomalies observed within the Oligocene and deeper Eocene also calibrate to thick sandstone units in the study area.

Sands overlay the mid-Miocene unconformity in CSS6 and pinches out away from a centre (Fig. 9). For the mound described above the Snorre Field in CSS7, sandstone units do not overlie the MMU directly, but are present within lower Pliocene sediments, before gradually pinching out into the mudstone dominated host strata (Fig. 10).

4. Origin and formation of emplacement of amplitude anomalies within the study area

Presented in the previous section are evidences of high-amplitude, discordant/concordant and mounded anomalies encased within low-amplitude background, extending from Cretaceous to Pliocene intervals similar to those observed in adjacent parts of the North Sea (Huuse *et al.* 2004). These anomalies are interpreted as products of sub-surface remobilization and injection of sands into low-permeable mudstones, which formed the Giant Sand Injection Complexes in the Northern North Sea based on the their spatial and temporal distribution with individual injectite sizes ranging from few hundreds to few kilometres. Sizes are often bigger (> 8 km) in complex injectites or individual injectites that have merged together. Other GISP

include Panoche, Faroe-Shetland basin, and other parts of the North Sea (Huuse *et al.* 2004; Hurst *et al.* 2006; Shoulder *et al.* 2007; Cartwright 2010; Løseth *et al.* 2013; Safronova *et al.* 2012; Monnier *et al.* 2014).

Interpretation was based on shape, geometries (cross section, plan view and 3D), dimensions, acoustic properties, and relationship of these high-amplitude, discordant anomalies with background mudstones; relationship with underlying structural elements and lithology. A summary of all the essential elements used to investigate these anomalies have been described in details in the previous section and also shown in table 3.

4.1 Timing of emplacement of amplitude anomalies and relationship with other elements within the study area

The actual timing of emplacement for sand injectites is not easy to constrain. In addition to calibration of age, quality and resolution of seismic data; constraining the timing depends on the nature of the injectite complex, i.e. whether it comprises of well-developed and preserved extrudites, acoustic impedance contrasts (between sands and shales), nature of subsequent sedimentation (pelagic or turbidites) and finally, assumptions based on current understanding of the injection process (whether wing tips reach seafloor or not). The extensive literature on sand injectites have estimated their timing, based on three (3) main criteria (Cartwright 2010), which will be used to estimate the timing in this study area.

Presence of an extrudite vented on the paleo-seafloor – Identifying an extrudite above sand injectites is very crucial, as it defines the position of seabed at the time of intrusion and extrusion (Huuse *et al.* 2004; Hurst *et al.* 2006; Vigorito *et al.* 2008). The surface, which an extrudite is emplaced on, or the seabed at the time of formation, pre-dates the extrudite and sediments that onlap onto an extrudite clearly post-dates it; suggesting emplacement is between the age of the seabed and the onlapping sediments. In the study area, we identified extrudite on the paleo-seafloor for those observed in CSS1 and CSS4, which provides clue to timing of their emplacement as mid to Late Paleocene and mid to Late Miocene respectively.

Termination of wings at a common datum – A stratigraphic datum, at which intrusions terminate, may have represented a paleo-seabed at the time of emplacement (Huuse et al. 2004). Ability to map and date the datum can provide estimation into timing of emplacement of intrusions. This is prone to misinterpretation where quality of seismic data is very poor and the datum is not mapped or dated correctly due to interference from polygonal faults or erosion. However, where this datum is clearly visible and mapped, this is a very good indication of timing. From the evidence in the previous section, we were able to clearly map common datum for injectites within CSS1 and CSS2 with these datum dated as Mid-Palaeocene and Mid-Eocene age respectively.

Dating of onlapped sediments – Forced folds or jack up, created above injectites, are onlapped by latter sediments. Dating the sediments that onlap on to the forced folds indirectly helps to estimate the timing of injectites (Shoulders *et al.* 2007; Cartwright 2010). We presented these forced folds and underlying injectite relationships in the previous section in CSS2 and CSS4 units.

Based on the three criteria above and evidences presented from each sequence in our study, we propose five (5) major episodes of emplacement in the NNS. They are: Late Cretaceous (CSS0), Middle Palaeocene (CSS1), Middle to Late Eocene (CSS2), Middle Miocene (CSS4 and CSS6) and Early Pliocene (CSS7). Some of the events are synchronous with other parts of the North Sea. For example, in the South Viking Graben, two episodic events are interpreted in the Early and Middle Eocene based on presence of extrusion and termination of conical intrusions at the unconformity respectively (Huuse *et al.* 2004). Middle to Late Eocene timing was also proposed for conical intrusions in the Tampen Spur area towards the western part of the Eocene-emplaced injectites case study (Huuse & Mickelson 2004). Rodriguez *et al.* (2009) also identified onlaps on forced folds above underlying sandstone intrusions during the mid-Miocene in the Tampen Spur area. Above the Siri Canyon in the Norwegian - Danish basin, an extrudite was interpreted on the mid-Miocene unconformity (Andresen *et al.* 2009). Examples mentioned above with our independent observations suggest the Middle Eocene and Middle Miocene times were periods of regional sand injectites emplacement in the whole of the North Sea.

What makes the study area very unique is the multiple occurrences of the sand injectite complexes through about 4000 m interval within the duration 95 Ma; compared to the single or two episodes interpreted in the other parts of the North Sea.

4.2 Parent bodies

Another important factor to consider in association with timing is the location of the parent bodies; evidences and discussions presented above suggested that the parent bodies that fed the Giant Sand Injectite Complex in the study area were located at multiple intervals similar to outcrop studies (Hurst & Cartwright 2007). Constraining the exact parent body for each intrusion complex is very challenging due to the complexity of the intrusion networks. Heavy mineral analysis on samples from both the intrusions and the depositional sand bodies could provide valuable information on sand and fluid source (Jonk 2010; Morton *et al.* 2014). Simplified sand distribution maps were re-drawn from previous and present study to show the extent of the depositional (yellow outlines) and post-depositional sandstone (red outlines) facies in the study area. The Shetlands and western Norway were the main sediment sources in the area. Laboratory experiments reveal that increase in pore pressure could cause fluidized sands to be forcefully injected into the host rock. Such that when sand and fluid mixture reaches a free surface or seabed, pressure is reduced and fluidized sands flows laterally away from the source point by gravity currents (Rodrigues *et al.* 2009; Ross *et al.* 2011). This could suggest why sandstone within the mound complexes observed in CSS6 and CSS7 often thin away from the centre of the mound (Figs. 9 & 10). These sands could have been sourced from underlying intervals (Huuse & Mickelson 2004; Løseth *et al.* 2013). Previous workers in the Snorre area, revealed presence of injectites in the underlying Oligocene interval and this study presents a similar interpretation for both examples in both case studies. We speculate that the injectites are connected to the overlying extrudites supplying sands onto the paleo seabed.

4.3 Sand injectites and underlying faults in the study area

Sand injectites have been interpreted above fault tips in previous studies as fluids may preferentially flow along faults (Cartwright 2010). An example of this is from the Barent Sea where sand injectites were interpreted above normal faults. These faults were suggested to have controlled the distribution and the faults served as pathways for deeper fluid migration into the parent sand bodies in the Eocene unit with both the sand injectites and faults having similar NNE-SSW orientation. (Safronova *et al.* 2012). Similar relationship was also observed in Faroe-Shetland Basin, such that sand injectites and underlying basement faults have same NE-SW trend (Shoulders *et al.* 2007). The North Sea basin was tectonically active in the Mesozoic time with series of normal faults, horst and grabens formed during the rifting and related to most of the major Jurassic oil and gas fields in the NNS (Ahmadi *et al.* 2003). Map of the base Cretaceous unconformity reveals the structural elements by highlighting structurally high areas from low areas, relay fault zones, fault linkage systems and graben step overs linked to underlying faulting and rifting (Fig. 12). The faults and structural highs have NNE-SSW orientation across the basin and locally coincide with distribution of some of the injectites in the area, which are distributed above or along the crest of these structural highs and fault planes. The mapped injectites are also present above structurally low areas and some of the structurally active zones (Troll faulted blocks) are devoid of intrusions; suggesting that structural element to sandstone intrusion relationship exist only locally.

4.4 Mechanism of Formation

Pre-requisite elements for formation of sandstone intrusions and extrusions include presence of unconsolidated sands emplaced within low-permeable mudstones, sufficient fluid to entrain the sands, excessive pore pressure and a triggering mechanism (Lonergan *et al.* 2000). Several authors have investigated different processes for formation of sandstone intrusions and extrusions but exact mechanism that initiated actual remobilization and injection are still very speculative. They are classified under primers and triggers; with the former constituting factors that generate the overpressure (liquefaction of the sands) and the latter as the processes that triggers the actual fluidization and injection (Huuse *et al.* 2010). Priming mechanisms include: disequilibrium compaction resulting in rapid burial of sand bodies and inability of pore fluids to escape normally (Osborne & Swarbrick 1997; Jackson *et al.* 2011; Løseth *et al.* 2013), hydrocarbon generation, lateral pressure transfer and fluid buoyancy (Yardley & Swarbrick 2000; Andresen *et al.* 2009; Monnier *et al.* 2014), migration of basinal fluids (Jolly & Lonergan 2002; Safronova *et al.* 2012), silica diagenesis (Davies *et al.* 2006; Huuse *et al.* 2010), tectonism due to basin inversion (Cartwright 2010) and a water-level drop (Hermanrud *et al.* 2013). These authors also suggested that triggering mechanisms that cause sand injectites to form could either be internally or externally driven such as differential compaction, lateral pressure transfer resulting in post-depositional tilting and migration of water and/or hydrocarbon into sealed sand bodies, seismic waves from large magnitude earthquakes, bolide impact, propagation of polygonal faults into overpressured sandstone bodies, buoyancy effects of hydrocarbons or faulting related to diapirism. All these processes were interpreted to prime or trigger emplacement of sand injectites during single episode of emplacement. We speculate that for such basin-scale remobilization and injection of sands as we have observed in our study area, a continuous or re-occurring mechanism will be more plausible for both over-pressure generation and trigger. Some of the known mechanisms mentioned above were investigated in our study.

Disequilibrium compaction resulting in rapid burial of sand bodies and inability of pore fluids to escape normally is a very common overpressure generation mechanism (Osborne & Swarbrick 1997; Jackson 2007). This mechanism is efficient when the seal integrity is very good and sedimentation rates are as high as or greater than 600 m /Ma (Durant & Hurst 2004; Osborne & Swarbrick 1997). Sedimentation rates, estimated in the study area from CSS0 to CSS9, are within the range of 24.10 and 415.63 m/Ma, for minimum and maximum rates observed in the CSS2 (Eocene) and CSS7 (Pliocene) units, respectively (Table 4, Olobayo *et al.* 2015 PhD thesis). Based on these low values (with the exception of the Pliocene ~600 m/Ma), disequilibrium compaction is not suggested as a plausible mechanism as sedimentation rates were not high enough to generate the required overpressure in the area. However, the rates in the Pliocene may have contributed at that time.

Another process that generates excess pressure is **high tectonic stresses**. Areas with applied tectonic stresses, such as strike-slip basins, fold and thrust belts have very high differential and applied stresses that can create excessive pressure (Lonergan *et al.* 2000). The North Sea is characterized by series of rift structures with the last phase of rifting between Late Jurassic to Early Cretaceous time (Ziegler 1990). By Late Cretaceous times, the North Sea was no longer actively rifting and the post-rift phase was characterized by thermal subsidence (Lonergan *et al.* 2000). The oldest intrusions in the NNS are observed in the Late Cretaceous interval, by then the area was no longer tectonically active (Lonergan *et al.* 2000); making tectonic stresses an unlikely mechanism for overpressure generation.

Addition of fluid, such as hydrocarbon, is another common mechanism, often sited in literature to generate overpressure in parent bodies of injectites (Lonergan *et al.* 2000; Jolly & Lonergan 2002; Duranti & Hurst 2004; Andresen *et al.* 2009; Wild & Briedis 2010; Monnier *et al.* 2014). This process is also thought to be very effective in remobilizing large volumes of unconsolidated sand and facilitate injection. Introduction of hydrocarbon, especially gas can generate high pore-fluid pressure in sealed sands, due to buoyancy (Jolly & Lonergan 2002; Duranti & Hurst 2004; Hurst *et al.* 2011). This is a very attractive mechanism for overpressure build up in the study area; firstly, because of the presence of underlying Late Jurassic Kimmeridge Clay source rock (age equivalent of Draupne Formation in the Norwegian Margin). Basin modelling shows hydrocarbon generation in the North Sea, started since the Late Cretaceous (Kubala *et al.* 2003). This is coeval with the timing of emplacement for the Late Cretaceous intrusions in the study area (Fig. 4). Secondly, the location of some of the intrusions above structural highs and Mesozoic faults, which houses most of the underlying reservoirs, suggests some kind of relationship between them (Fig. 12). However, not all intrusions are present on structural highs and faults, as they are also observed within the structurally low areas and not present above some structural highs, such as the Troll fault blocks. Some of the intrusions mapped in the area also occur in areas not underlained by hydrocarbon fields. Therefore, this mechanism alone might not be sufficient enough to trigger remobilization and injection due to only partial correlation between underlying structures and mapped injectites.

Recently, the process of opal A to opal CT silica diagenetic transformation was invoked as a potential primer and trigger for sandstone intrusions (Davies *et al.* 2006). The conversion, which often occurs at shallow burial (first 0.5 - 1 km), causes collapse of the pore framework, drastic porosity loss and rapid pore fluid

expulsion, which facilitates generation of abnormally high pressure within the unit. This study favours this mechanism based on the following:

Evidence of multiple emplacements of sand injectites in the NNS, these includes: Late Cretaceous, Middle Paleocene, Middle to Late Eocene, Middle to Late Miocene and Early Pliocene.

Evidence of transformation of opal A to opal CT within Paleocene, Eocene and Oligocene intervals from seismic, well data and petrophysical analysis (Rundberg 1991).

Location of present day boundary of diagenetic boundary below Oligocene-emplaced injectites (observations from seismic and well logs) (Figs. 7 - 10).

Presence of potential parent sand bodies for the intrusions located within opal-rich interval in the study area.

Average depths at time of injection are between 300 – 600 m in the area (for sand injectites of about 200 m to 400 metres in height) and since diagenesis have been known to occur within the first 0.5 - 1 km (Davies *at al.* 2006); this means that both processes occurred at similar depths.

Nature of the host rock – presence of extensive polygonal fault system developed in Cretaceous to Miocene aged sediments is evidence of early dewatering. Mudstones are also smectitic-rich and have undergone transformation to illite (Rundberg 1991) and could have provided addition fluid into the system. Diagenetic processes result in shear fracturing in fine-grained sediments.

Finally, the co-existence of opal-rich rock and sandstone intrusions is very compelling in the North Sea, Faroe-Shetland Basin, Sakhalin Island, More Basin and San Joaquin Basin (Davies *et al.* 2006; Thompson *et al.* 2007).

The main fluid sources that could have driven such a large-scale remobilization and injection in the NNS are: intraformational fluid sources, such as diagenesis of the host rock, compaction and extraformational fluid sources, such as hydrocarbon or/and water from deeper parts of the basin. For such scale of remobilization, a basinal event might be needed to trigger it, i.e regional events like earth quakes or bolide impacts (Obermier 1989; Huuse *et al.* 2010). Earthquakes have been proposed to trigger remobilization and injection of unconsolidated sand by a process known as shear-induced liquefaction or dynamic liquefaction. These studies reveal that earthquake events may create shearing motion within the rock, which leads to grain crushing, causing significant increase in fluid pressure, weakening of overburden rocks and causing injection (Obermier 1989). However, this is known to occur at very shallow depth (within few metres of the surface) and produces centimetres to few metres structures (Obermier 1996; Cartwright 2010). Jolly & Lonergan (2002) also noted that at greater depth, it is difficult to liquefy sediments by dynamic liquefaction, due to increase in overburden stress with depth. The scale of intrusion, depth of intrusion and magnitude of earthquake should also be considered, when invoking seismically-induced liquefaction as a potential driving mechanism for intrusions (Jolly & Lonergan (2002). In the study area, the scale of intrusions is in hundreds and thousands of magnitudes larger than those formed by seismically-induced liquefaction. Depths of intrusion in the area are assumed to be within the range of 400 – 600 m, therefore too deep for dynamic liquefaction. Lastly, no known record of

earthquakes with magnitudes > 5 is known in the area (Huuse & Mickelson 2004). Based on the above, the study does not favour earthquakes as a possible triggering mechanism in the area.

Bolide impact, which created the Silver Pit crater in the southern North Sea and the Ries impact in Germany during the mid to Late Eocene and mid to Late Miocene, respectively, was also suggested in literature as potential triggers for sandstone intrusions (Cartwright 2010). Although the timing of these events coincides with timing of emplacement of some of the intrusions in the area, they occurred at great distances away from the study area and their impact is not expected to have reached the NNS making the process unlikely.

6. Conclusions

The study forms part of the North Sea intrusion province described by Cartwright (2010). Other similar examples of large-scale injectites are the Faroe-Shetland and Paonoche - Tumey complexes. Based on this study, the following conclusions are presented below:

Presence of series of high–amplitude, anomalies emplaced within low-amplitude background pervasively deformed by polygonal faults at multiple intervals in the area from Cretaceous to Pliocene

Three main styles were described: (i) high-amplitude, bedding-discordant which have V, U or W- shape geometries (ii) high-amplitude, bedding-concordant and (iii) steep-mounded anomalies

Some of the anomalies penetrated by exploration wells encountered tens of metres thick sandstones and interpreted as sandstone intrusions and extrusions

Five (5) episode of emplacement occurred from Late Cretaceous to Early Pliocene in the NNS

Occurrence of multiple tiers of polygonal fault networks within fine-grained, smectite-rich and siliceous-rich mudstones from Cretaceous to Miocene intervals

Evidence of silica diagenetic transformation at multiple intervals (Paleocene-Oligocene)

Transformation of opal A to opal CT results in abrupt porosity loss, significant water expulsion and excessive pore pressure. This process is proposed as a potential driving mechanism for intrusion emplacement, combined with hydrocarbon generation. Pore water expelled during conversion, hydrocarbon and pore water from other processes are considered as fluid sources for fluidization of the intrusions in the area

Sealed unconsolidated sands could have subsided through the transformation zones with intrusions emplaced at multiple intervals through time

Potential parent bodies are depositional sandstones in form of fans and channels also located at different stratigraphic levels

Local occurrences between sand injectites and underlying structural elements suggest they could have influenced their distribution. Hydrocarbon maturation in the area started in Late Cretaceous and continues till date, coinciding with timing of oldest intrusion (CSS0)

Multiple stratigraphic occurrences in the study area could have impacted prospectivity in the Tertiary interval of the NNS as their presence is evidence of breach in the sealing rocks.

The study represents the first-ever, documentation of large-scale sand injectites emplaced during series of episodic events in a single basin. Main episodes proposed include: Late Cretaceous, Middle Palaeocene, Middle to Late Eocene, Middle Miocene and Early Pliocene. This is useful in calibrating fluid and fluid flow history in the basin during reservoir modelling (Shoulders et. Al. 2007). Therefore, there is need to incorporate them into the present Cenozoic framework in the NNS and other basins in the world. Figure 13 shows a schematic section across the Northern, Central and Southern sections across the study area with underlying Jurassic faults to show approximate lateral and vertical distribution of intrusions. Also shown are locations of polygonal faults and silica diagenetic transformation zones. shows a (Fig. 13).

Acknowledgements

The authors wish to thank PGS for providing the 3D MegaSurvey seismic volume which most of this interpretation was based on and TGSNOPEC for proving regional 2D seismic lines for this project. Gratitude goes also to Norwegian Petroleum Directorate (NPD.NO) website for information on the wells used. Appreciation also goes to the reviewers for their constructive comments in the process of reviewing this paper.

Funding

Special appreciation to the Petroleum Technology Development Fund (PTDF) of Nigeria for providing full funding for this research project.

References

AHMADI, Z.M. SAWYERS, M. KENYAN-ROBERTS, S. STANWORHT, C.W. KUGLER, K.A. KRISTENSEN, J. & FUGELLI, E.M.G. (2003). Palaeocene. In: *The Millennium Atlas: Petroleum geology of the central and northern North Sea* (Ed. by D. Evans, C. Graham, A. Armour & P. Bathurst). *The Geological Society of London, London*, 235–259.

ANDRESEN, K. J. CLAUSEN, O. R. & HUUSE, M. (2009). A giant (5.3x107m^3) middle Miocene (c. 15Ma) sediment mound (M1) above the Siri Canyon, Norwegian-Danish Basin: origin and significance. In press: *Marine and Petroleum Geology.*

BUREAU, D. MOURGUES, R. CARTWRIGHT, J. FOSCHI, M. & ABDELMALAK, M.M (2013). Characterisation of interactions between a pre-existing polygonal fault system and sandstone intrusions and the determination of paleo-stresses in the Faroe-Shetland basin. *Journal of Structural Geology, 46,* 186-199

CARTWRIGHT, J.A. (2010). Regionally extensive emplacement of sandstone intrusions: a brief review. *Basin Research, 22, 502 – 516*

DAVIES, R. J. HUUSE, M. HURST, P. CATWRIGHT, J. & YANG, Y. (2006). Giant clastic intrusions primed by silica diagenesis. *Geology, 34,* 917-920.

DURANTI, D. & HURST, A. (2004). Fluidization and Injection of deepwater sandstones of the Eocene Alba Formation (UK North Sea). *Sedimentology, 51,* 503-529.

GOLEDOWSKI, B. NIELSEN, S.B. & CLAUSEN, O.R. (2012) Patterns of Cenozoic sediment flux from western Scandinavia. *Basin Research, 24,* 377–400

GOULTY, N.R (2001). Polygonal fault networks in fine-grained sediments an alternative to the synthesis mechanism. *First break 19,* 69-73

HERMANRUD, C. VENSTAD, J . M. CARTWRIGHT, J. RENNAN, L. HERMANRUD, K. & BOLÅS, H. M. N. (2013). Consequences of Water Level Drops for Soft Sediment Deformation and Vertical Fluid Leakage. *International Association for Mathematical Geosciences, 45, 1-30*

HURST, A. & CARTWRIGHT, J. (Eds.) (2007). Sand Injectites: Implications for Hydrocarbon Exploration and Production, *AAPG Memoir, 87*. AAPG, Tulsa.

HURST, A., CARTWRIGHT, J., HUUSE, M., AND DURANTI, D. (2006). Extrusive sandstones (extrudites): a new class of stratigraphic trap? In: The Deliberate Search for Stratigraphic Traps: Where Are They Now? (Eds M.R. Allen, G.P. Goffey, R.K. Morgan and I.M. Walker), *Geological Society London, Special Publication 254,* 289–300.

HURST, A., SCOTT, A. & VIGORITO, M. (2011).Physical characteristics of sand injectites. *Earth-Science Reviews, 106,* 215-246.

HURST, A., HUUSE, M., DURANTI, D., JAMESON, E. & SCHWAB, A. (2016). Application of outcrop analogues in successful exploration of a sand injection complex, Volund field, Norwegian North Sea, In Bowman, M., (Ed.), *Geological Society, London, Special Publications, 436,* 75-92.

HUUSE, M. CARTWRIGHT, J. HURST, A. &STEINSLAND, N. (2007) Seismic characterization of large-scale sandstone intrusions. In: Sand Injectites: Implications for Hydrocarbon Exploration and Production (Ed. by A. Hurst & J. Cartwright), *AAPG Memoir. 87,* 21-35.

HUUSE, M. DURANTI, D. STEINSLAND, N. GUARGENA, C.G. PRAT, P. HOLM, K. CARTWRIGHT, J.A. & HURST, A. (2004). Seismic characteristics of large-scale sandstone intrusions in the Paleogene of the South Viking Graben, Uk and Norwegian North Sea. In R. J. Davies, J. Cartwright, S. A. Stewart, J. R. Underhill, & M. Lappin (Eds.), *3D seismic technology: application to the exploration of sedimentary basins. Geological Society, London Memoir, 29,* 257-271

HUUSE, M. JACKSON, C.A.-L. RENSBERGEN, P. V. DAVIES, R.J. FLEMINGS, P.B. & DIXON, R.J. (2010) Subsurface sediment remobilization and fluid flow in sedimentary basins: an overview: *Basin Research, 22,* 342-360.

HUUSE, M. & MICKELSON, M. (2004). Eocene sandstone intrusions in the Tampen Spur area (Norwegian North Sea Quad 34) imaged by 3D seismic data. *Marine & Petroleum Geology, 21*, 141-155.

ISAKSEN, D. & TONSTAD, K.E. (1989) A revised Cretaceous and Tertiary lithostratigraphic nomenclature for the Norwegian North Sea. *Norwegian Petroleum Directorate (NPD) Bulletin, 5*, 1–59.

JACKSON, C.A.L (2007). The geometry, distribution, and development of clastic injections in slope systems: seismic examples from the Upper Cretaceous Kyrre Formation, Maloy Slope, Norwegian Margin. *In: Sand Injectites: Implications for Hydrocarbon Exploration and Production (ed. By A. Hurst & J. Cartwright), AAPG Memoir, 87*, 37-48.

JACKSON, C. A. L. & SOMME, T. O. (2011). Borehole evidence for wing-like clastic intrusion complexes on the western Norwegian margin. *Journal of the Geological Society, 168, 1075-1078*

JENKINS, O.P. (1930). Sandstone dikes as conduits for oil migration through shales. *AAPG Bulletin, 14,* 411-421.

JOLLY, R.J.H. &LONERGAN, L. (2002). Mechanisms and controls on the formation of sand intrusions. *Journal of the Geological Society, 159,* 605-617

JORDT, H. THYBERG, B.I. & NØTTVEDT, A. (2000) Cenozoic evolution of the Central and Northern North Sea with focus on differential vertical movements of the basin floor and surrounding clastic source areas. In: Dynamics of the Norwegian margin (Ed. by A. Nøttvedt) *Geological Society London, Special Publication,* 167, 219–243.

KUBALA, M. BASTOW, M. THOMPSON, S. SCOTCHMAN, I. OYGARD, K. (2003). Geothermal regime, petroleum generation and migration. In: Evans, D. Armour, C.G.A. Bathurst, P. (Eds.), The Millennium Atlas: Petroleum Geology of the Central and Northern North Sea. The Geological Society of London, London, pp. 289–315.

LONERGAN L. LEE N. JOHNSON, D.H. CARTWRIGHT, A.J. JOLLY, J.H.R. (2000). Remobilization and injection in deep water depositional systems: implications for reservoir architecture and prediction. *Gcssepm foundation 20th annual research conference.*515-531.

LØSETH, H. RAULINE, B. & NYGARD, A. (2013). Late Cenozoic geological evolution of the northern North Sea: development of a Miocene unconformity reshaped by large-scale Pleistocene sand intrusion. *Journal of the Geological Society,170,* 133-145

MARTINSEN, O.J. BØEN, F. CHARNOCK, M.A.MANGERUD, G. & NØTTVEDT, A. (1999) Cenozoic development of the Norwegian margin 60-64ºn: Sequences and sedimentary response to variable basin physiography and tectonic setting. In: Petroleum Geology of Northwest Europe: Proceedings of the 5th Conference (Ed. by A.J. Fleet & S.A. Boldy). *Geological Society London, London,* 293-304

MONNIER, D. IMBERT, P. GAY, A. MOURGUES, R. & LOPEZ, M. (2014). Pliocene sand injectites from a submarine lobe fringe during hydrocarbon migration and salt diapirism: a seismic example from the Lower Congo Basin. *Geofluids 14, 1-19.*

MORTON, A. MCFADYEN, S. HURST, A. PYLE, J. & PHILIP, R. (2014). Constraining the origin of reservoirs formed by sandstone intrusions: Insights from heavy mineral studies of the Eocene in the Forties area, United Kingdom central North Sea. *AAPG Bulletin, 98,* 545-561

OLOBAYO, O. HUUSE, M. & JACKSON, C. A. L. (2015). PhD Thesis - Deposition, Remobilization and Fluid Flow in Sedimentary Basins – Case Studies in the Northern North Sea and Nigeria Transform Margin

ROSS, J.A. PEAKALL, J. & KEEVIL, G.M (2011).An integrated model of extrusive sand injectites in cohesionless sediments. *Sedimentology 58,* 1693-1715

RUNDBERG, Y. (1991) Tertiary sedimentary history and basin evolution of the Norwegian North sea between 60 – 62 degrees N – an Integrated Approach. *PhD Thesis, University of Trondheim.*

RUNDBERG, Y. & EIDVIN, T. (2005) Controls on depositional history and architecture of the Oligocene-Miocene succession, northern North Sea Basin. *Norwegian Petroleum Society, Special Publication, 12,* 207–239.

SAFRONOVA, P.A. ANDREASSEN, A. LABERG, J.S. & VORREN, T.O. Development and post-depositional deformation of a Middle Eocene deep-water sandy depositional system in the Sørvestsnaget Basin, SW Barents Sea. *Marine and Petroleum Geology, 36,* 2012 83-99

SHOULDERS, S.J. CARTWRIGHT, J. & HUUSE, M. (2007). Large scale conical sandstone intrusions and polygonal fault systems in Tranche 6, Faroe-Shetland basin. *Marine & Petroleum Geology, 24,* 173-188.

SCHWAB, A.M., JAMESON, E.W., & TOWNSLEY, A. (2014). Volund Field: development of an Eocene sandstone injection complex, offshore Norway, in MacKie, T. (Ed.), *Geological Society, London, Special Publications,403,* 247-260

THOMPSON, B.J.GARRISON, R.E.&MOORE, J.C. (2007)A reservoir-scale Miocene Injectite near Santa Cruz, California. In: Sand Injectites: Implications for Hydrocarbon Exploration and Production (Ed. by A. Hurst & J. Cartwright). *AAPG Memoir, 87.* 151-162.

THYBERG, B. JAHREN, J. WINJE, T. BJØRLYKKE, K. FALEIDE, J.I. & MARCUSSEN, Ø. (2010). Quartz cementation in Late Cretaceous mudstones, northern North Sea: Changes in rock properties due to dissolution of smectite and precipitation of micro-quartz crystals. Marine an d *Petroleum Geology, 27,* 1752-1764

VIGORITO, M. HURST, A. CARTWRIGHT, J. SCOTT, A. (2008). Regional-scale subsurface sand remobilization: geometry and architecture. *Journal of Geological Society 165,* 609–612.

WILD, J. & BRIEDIS, N. (2010).Structural and stratigraphic relationships of the Paleocene mounds of the Utsira High. *Basin Research, 22, 533-547.*

YARDLEY, G.S. &SWARBRICK, R.E. (2000) Lateral transfer: a source of additional overpressure? *Marine and Petroleum Geology,17,* 523-537.

ZIEGLER, P.A. (1990) Collision related intra-plate compression deformations in western and central Europe. *Journal of Geodynamics,* 11, 13, 771–780.

Figure and Table captions

Fig. 1. Structural map of the North Sea basin showing major structures such as the triple arm, highs, sub-basins, terraces, platforms, faults and surrounding landmasses (modified from Fraser *et al.* 2003). Location of study area is shown in the red outline. MB-Magnus Basin, ESB-East Shetland Basin, ESP-East Shetland Platform, TS-Tampen Spur, SG-Sogn Graben, MT-Maloy Terrace, UT-Uer Terrace, LT-Lomre Terrace, HP-Horda Platform, OFZ-Øygarden Fault Zone, SB-Stord Basin, FGS-Fladen Ground Spur, UH-Utsira High, WGG-Witch Ground Graben, OMF-Outer Moray Firth, IMF-Inner Moray Firth, RFH-*Ringkøbing* Fyn-High, MNSH-Mid North Sea High. Also included on the map are locations of some hydrocarbon producing fields/discoveries. Yellow numbered squares represents fields associated with remobilised/injected sands (1-Kraken, 2-Jotun, 3-Grane, 4-Mariner, 5-Leadon, 6-Volund, 7-Gryphon, 8-Harding, 9-Balder, 10-Sleipner, 11-Alba, 12- Chestnut, 13-Forties, 14-catcher, 15-Cecile, 16-Siri, 17-Nini). Yellow stars show locations of previous work done in the area that are related to post-depositional products or soft-sediment deformation. Inset shows present day bathymetry of the North Sea. Black and red outline show location of the whole the North Sea and study area respectively

Fig. 2. (a) NW-SE trending seismic and (b) geo-seismic section showing mapped sequences, surfaces, internal characteristics of the units, underlying structural highs and faults. White horizon represents the opal A to opal CT diagenetic boundary cutting across the Oligocene succession.

Fig. 3. Mapped intrusions overlained with TWT thickness maps (ms) of individual sequences **(a)** CSS0 – Cretaceous (**b)** CSS1 - Paleocene **(c)** CSS2 - Eocene **(d)** CSS4 - Oligocene **(e)** CSS6 – Miocene-Pliocene injectite distribution overlay for all sequences.

Fig. 4. (a) Maximum amplitude between top Turonian and Cenomanian horizons to image channels and upper Cretaceous fan **(b&c)** TWT map of the top Turonian showing polygonal faults and zoom on the channels **(d-f)** dip lines showing discordant wings along channels **(g)** strike line. c and d represents concordant and discordant respectively

Fig. 5. Mound **(a&b)** uninterpreted and interpreted seismic sections of mound **(c)** seismic sections to show underlying possible feeders **(d)** TWT (ms) of mound

Fig. 6. CSS2 anomalies (**a&b)** strike and dip sections with well log calibration through high-amplitude, discordant anomalies around the Gullfaks area. **(c)** well calibration of anomalies **(d)** time slices through single anomaly. Slices reveal circular plan view geometry. **(e)** time-slice @ 1772 ms showing 3D conical and circular plan view geometry of the anomalies **(f)** 3D image showing spatial distribution of Eocene injectites along the crest of the structural highs **(g)** RMS amplitude at 150 ms above the top Balder surface.

Fig. 7. CSS4 anomalies (**a)** Seismic section and well calibration through the Eocene fans. Note presence of amplitude anomalies at the fringe and above the fans. Well 35/8-2 penetrated an anomaly above opal A to opal CT boundary **(b)** zoom to show well calibration **(c)** TWT thickness map (ms) of the Eocene fans

Fig. 8. (a) Single, mounded anomaly observed on the MMU and underlying saucer-shaped anomaly **(b**) zoom on saucer-shaped anomaly and mound to show notable jackup of the horizons similar to the Volund structure. W – wings, S – sill, P – pockmark.

Fig. 9 (a&b) Seismic and well log calibration showing mounded morphology of the MMU and its relationship with underlying high-amplitude discordant anomalies **(c&d)** TWT map of the MMU (**e)** TWT thickness map of the MMU and top horizon **(f)** variance amplitude map of the TWT map of the MMU

F**ig. 10.** Seismic section with well log calibration above the Snorre Field showing sand distribution in the area. Sands within Pliocene mudstones are interpreted as extrudites

Fig. 11. a-e Simplified sand distribution maps re-drawn from previous and present study, showing depositional (yellow outlines) and post-depositional sandstone (red outlines) facies. Main sediment sources are the Shetlands and western Norway.

Fig. 12. Outline of intrusions in the study area above a variance map of the base Cretaceous unconformity to show the relationship between the intrusions and underlying structural elements. Each phase is represented by a colour as shown in the legend. Note that intrusions occur above structural highs, along crest of highs, above fault planes as well as with the lows. Red lines represent underlying fields and discoveries. Distribution of intrusions appears to follow dominant NNE-SSW orientation of the underlying Mesozoic faults. Note stratigraphic overlap between intrusion complexes

Fig. 13. Northern, central and southern sections across the study area with underlying Jurassic faults to show approximate lateral and vertical distribution of intrusions. Also shown are locations of polygonal faults and silica diagenetic transformation zones.

Table 1 Summary of geometrical characteristics of sandstone injectites observed in the Cenozoic Northern North Sea basin

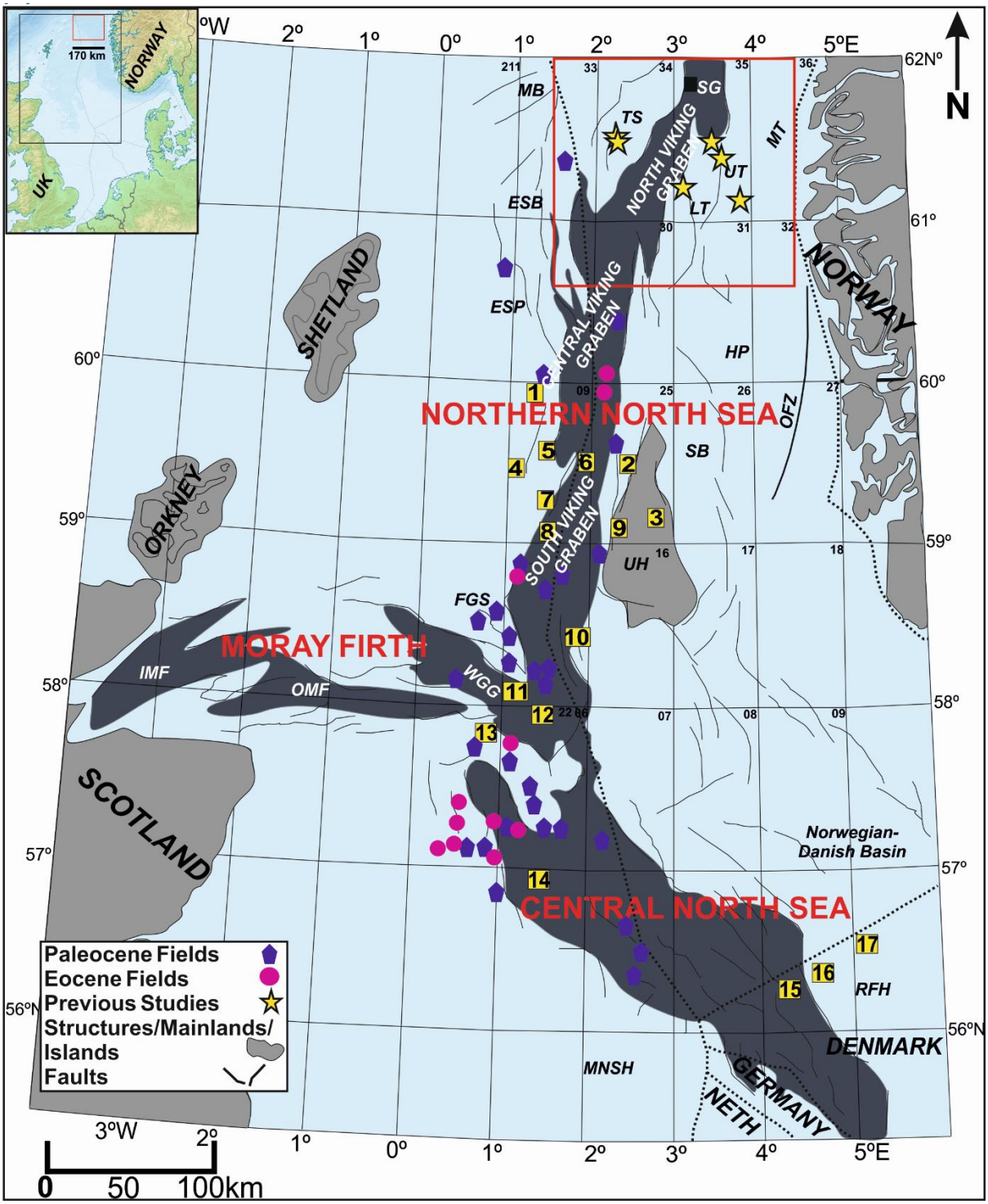
170 km
NORWAY
UK
°W
2°
1°
0°
1°
2°
3°
4°
5°E
62N°
61°
60°
59°
58°
57°
56°N
N
MB
ESB
ESP
SG
TS
UT
LT
MT
NORTH VIKING GRABEN
CENTRAL VIKING GRABEN
SOUTH VIKING GRABEN
SHETLAND
ORKNEY
SCOTLAND
NORWAY
HP
SB
OFZ
UH
FGS
WGG
IMF
OMF
MORAY FIRTH
NORTHERN NORTH SEA
CENTRAL NORTH SEA
Norwegian-Danish Basin
RFH
DENMARK
GERMANY
NETH
MNSH
1
2
3
4
5
6
7
8
9
10
11
12
13
14
15
16
17
Paleocene Fields
Eocene Fields
Previous Studies
Structures/Mainlands/Islands
Faults
3°W
2°
1°
0°
1°
2°
3°
4°
5°E
0
50
100km

Fig. 1

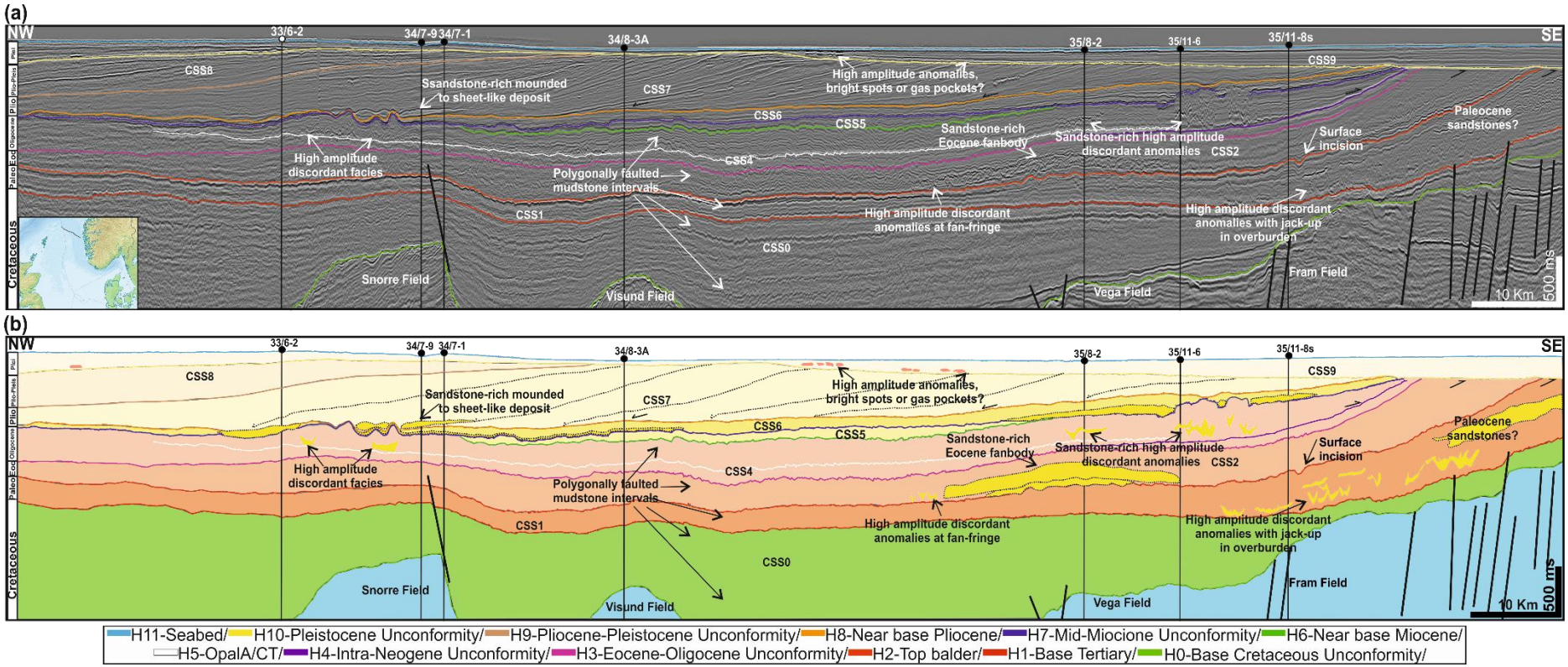

Fig. 2

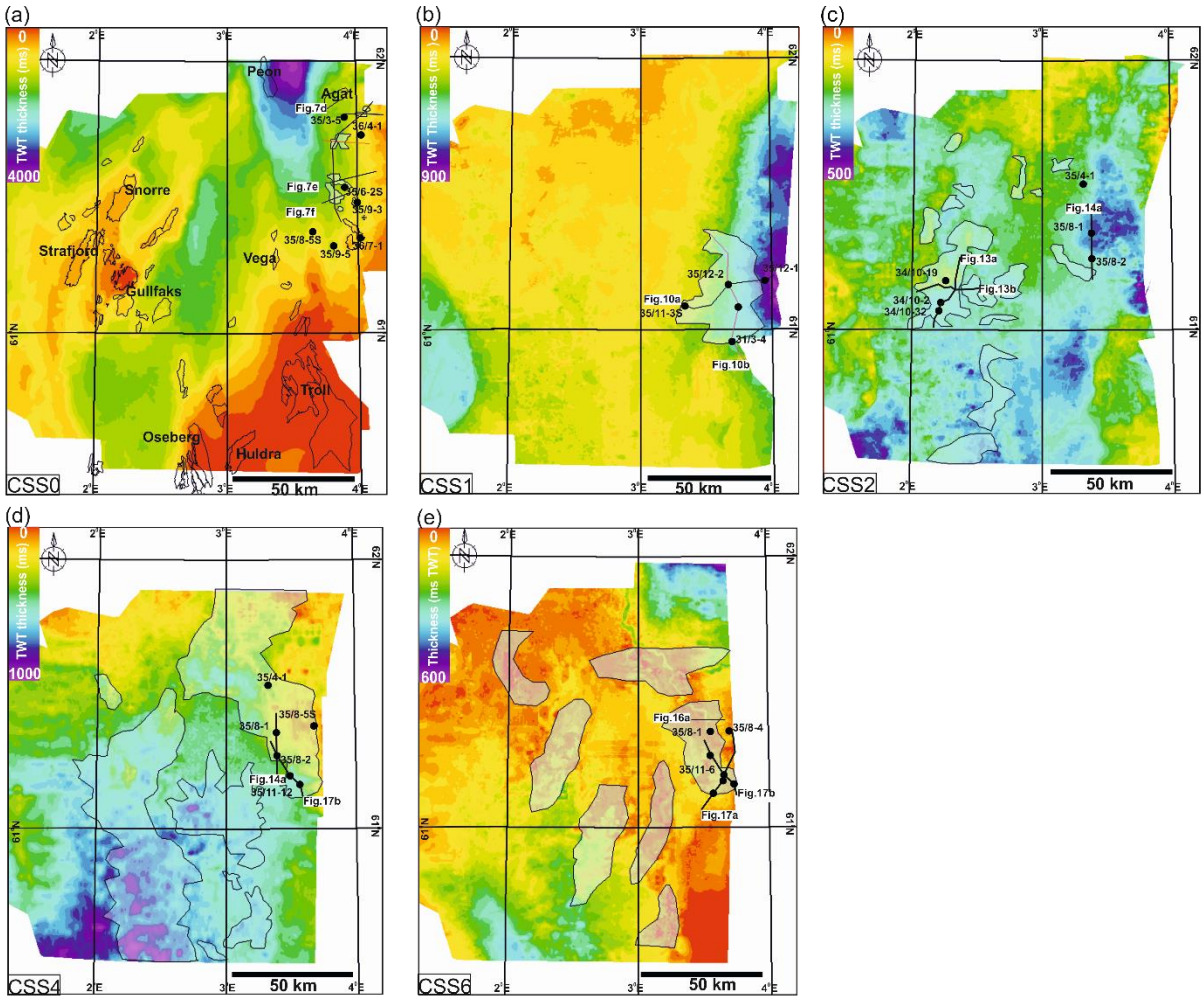
(a)
TWT thickness (ms)
0
4000
Peon
Agat
Fig.7d
35/3-5
16/4-1
Snorre
Fig.7e
35/6-2S
Fig.7f
35/9-3
35/8-5S
35/9-5
35/7-1
Strafjord
Vega
Gullfaks
Troll
Oseberg
Huldra
CSS0
50 km
(b)
TWT Thickness (ms)
0
900
35/12-2
35/12-1
Fig.10a
35/11-3S
31/3-4
Fig.10b
CSS1
50 km
(c)
TWT thickness (ms)
0
500
35/4-1
Fig.14a
35/8-1
35/8-2
Fig.13a
34/10-19
Fig.13b
34/10-2
34/10-32
CSS2
50 km
(d)
TWT thickness (ms)
0
1000
35/4-1
35/8-5S
35/8-1
35/8-2
Fig.14a
35/11-12
Fig.17b
CSS4
50 km
(e)
Thickness (ms TWT)
0
600
Fig.16a
35/8-1
35/8-4
35/11-6
Fig.17b
Fig.17a
CSS6
50 km

Fig. 3

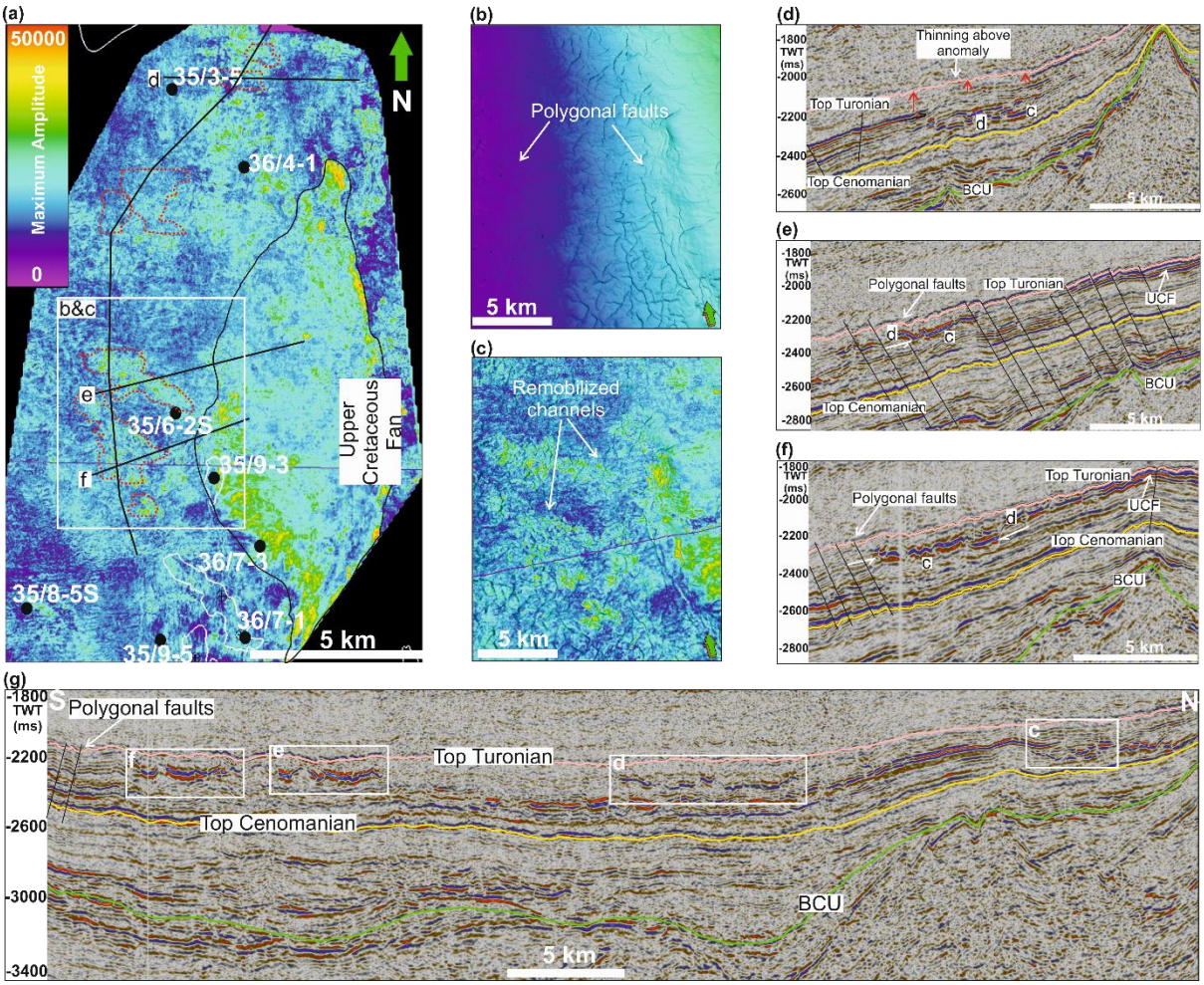

Fig. 4

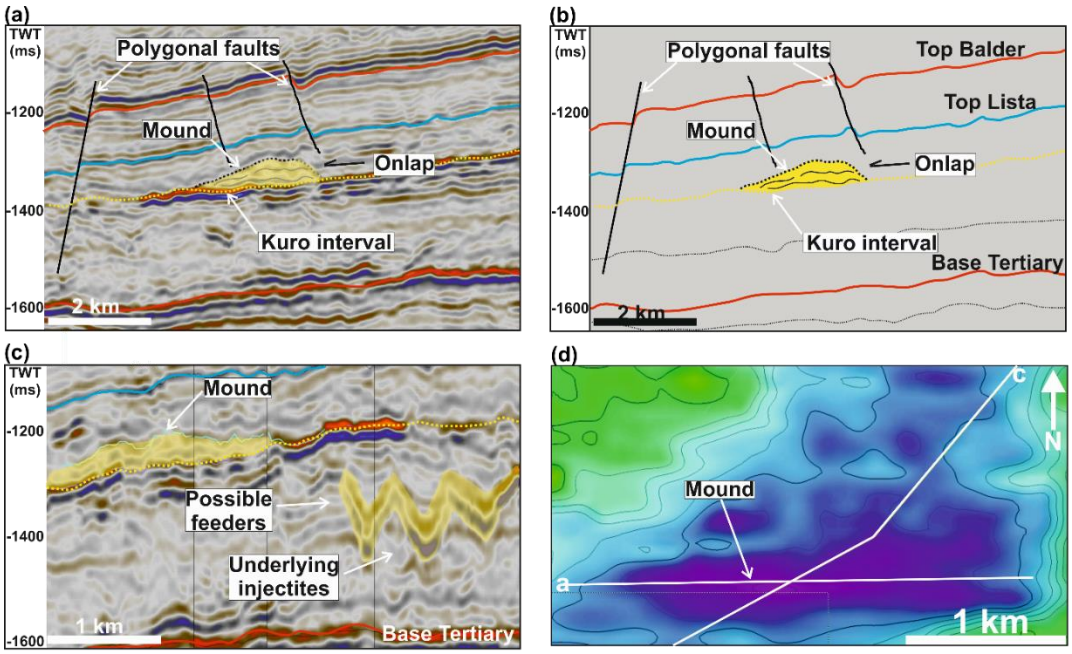
(a)
TWT (ms)
-1200
-1400
-1600
Polygonal faults
Mound
Onlap
Kuro interval
2 km
(b)
TWT (ms)
-1200
-1400
-1600
Polygonal faults
Top Balder
Top Lista
Mound
Onlap
Kuro interval
Base Tertiary
2 km
(c)
TWT (ms)
-1200
-1400
-1600
Mound
Possible feeders
Underlying injectites
1 km
Base Tertiary
(d)
c
N
Mound
a
1 km

Fig. 5

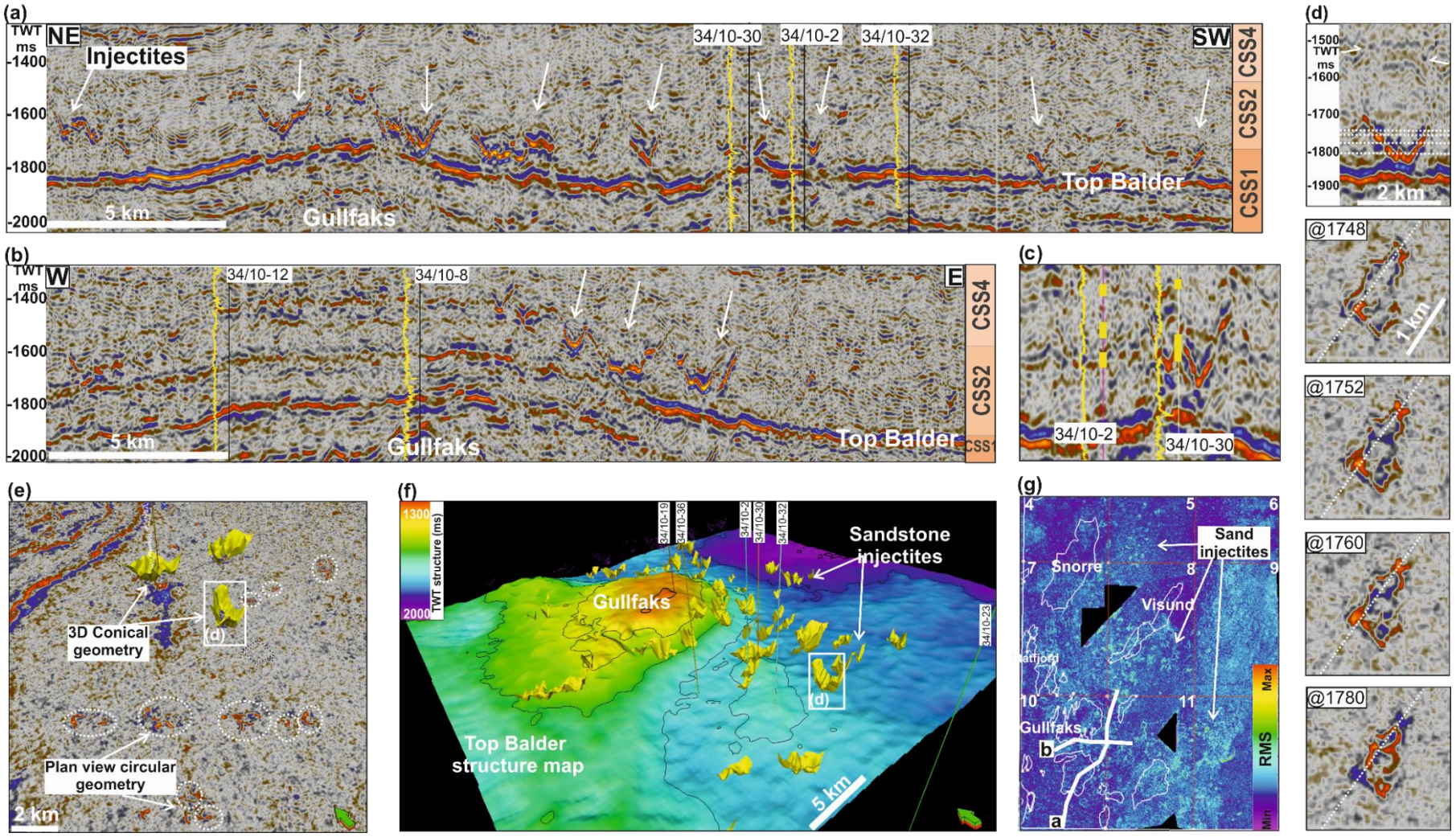

Fig. 6

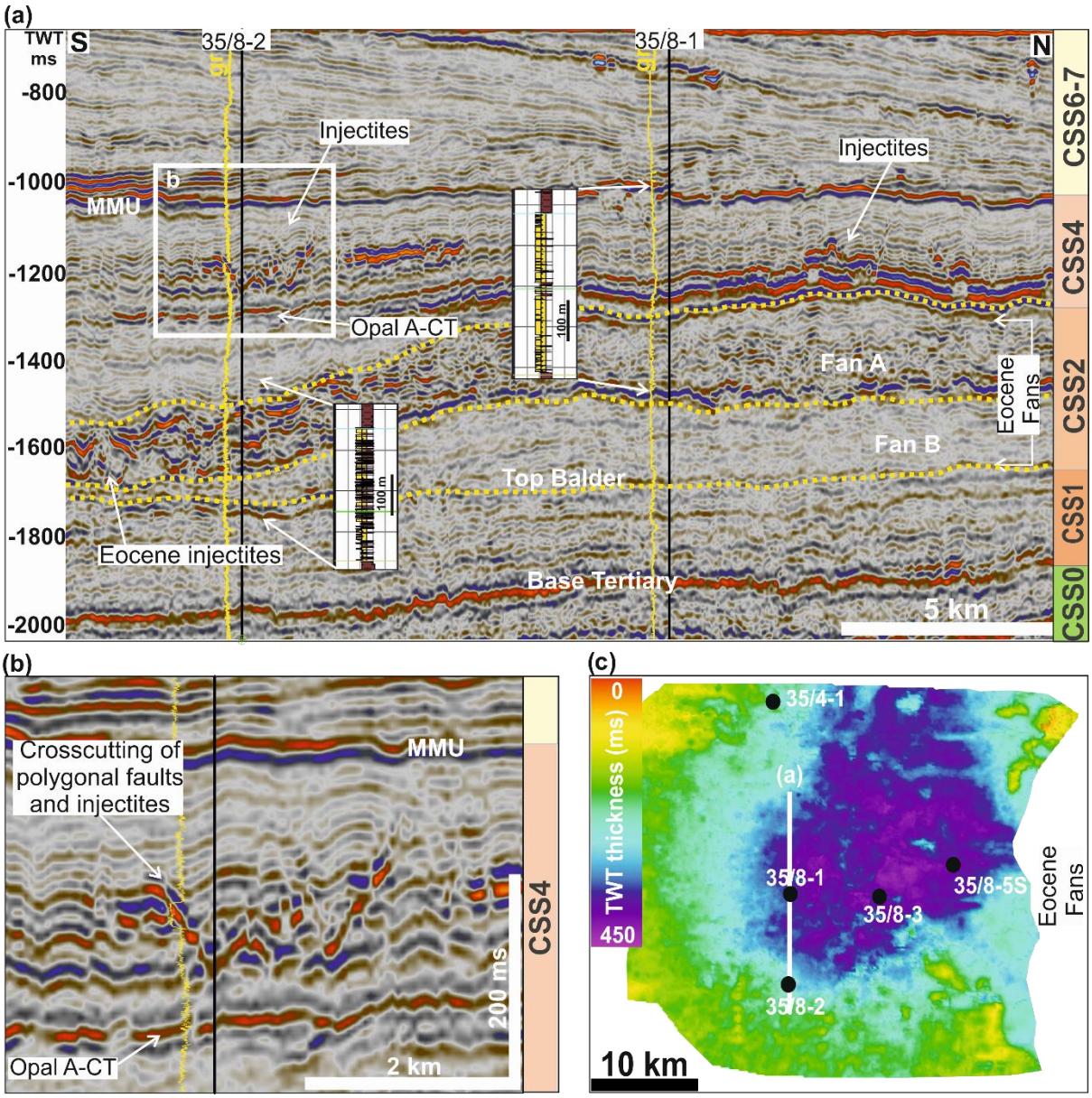
(a)
TWT ms
S
35/8-2
35/8-1
N
-800
-1000
-1200
-1400
-1600
-1800
-2000
MMU
b
Injectites
Injectites
Opal A-CT
Fan A
Fan B
Eocene Fans
Top Balder
Eocene injectites
Base Tertiary
5 km
CSS6-7
CSS4
CSS2
CSS1
CSS0
100 m
(b)
Crosscutting of polygonal faults and injectites
MMU
CSS4
200 ms
Opal A-CT
2 km
(c)
0
TWT thickness (ms)
450
35/4-1
(a)
35/8-1
35/8-5S
35/8-3
35/8-2
Eocene Fans
10 km

Fig. 7

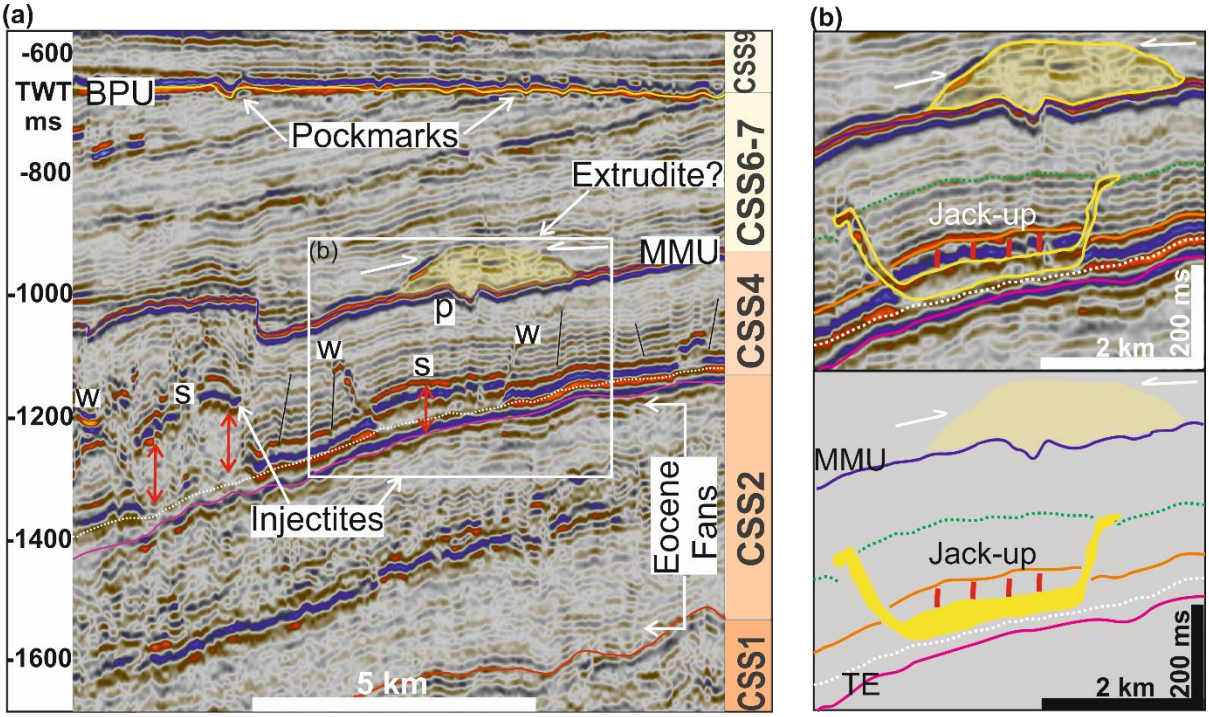
(a)
-600
TWT ms
-800
-1000
-1200
-1400
-1600
BPU
Pockmarks
Extrudite?
MMU
(b)
p
w
s
w
s
w
Injectites
Eocene Fans
5 km
CSS9
CSS6-7
CSS4
CSS2
CSS1
(b)
Jack-up
2 km
200 ms
MMU
Jack-up
TE
2 km
200 ms

Fig. 8

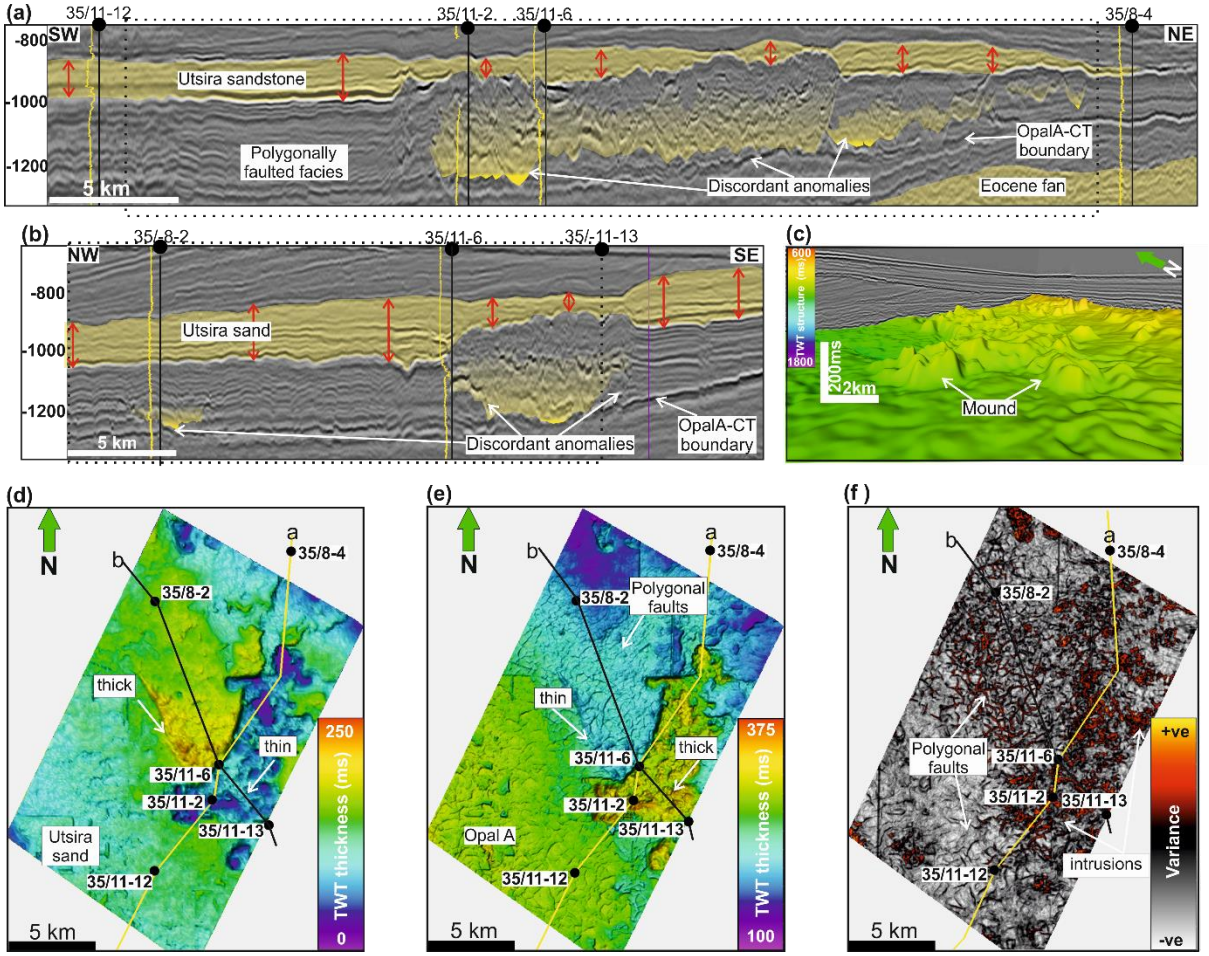
(a)
35/11-12
35/11-2
35/11-6
35/8-4
SW
NE
-800
-1000
-1200
Utsira sandstone
Polygonally faulted facies
Discordant anomalies
OpalA-CT boundary
Eocene fan
5 km
(b)
35/8-2
35/11-6
35/-11-13
NW
SE
-800
-1000
-1200
Utsira sand
Discordant anomalies
OpalA-CT boundary
5 km
(c)
600
TWT structure (ms)
1800
200ms
2km
Mound
(d)
N
a
35/8-4
b
35/8-2
thick
thin
35/11-6
35/11-2
35/11-13
Utsira sand
35/11-12
250
TWT thickness (ms)
0
5 km
(e)
N
a
35/8-4
b
35/8-2
Polygonal faults
thin
thick
35/11-6
35/11-2
35/11-13
Opal A
35/11-12
375
TWT thickness (ms)
100
5 km
(f)
N
a
35/8-4
b
35/8-2
Polygonal faults
35/11-6
35/11-2
35/11-13
intrusions
35/11-12
+ve
Variance
-ve
5 km

Fig. 9

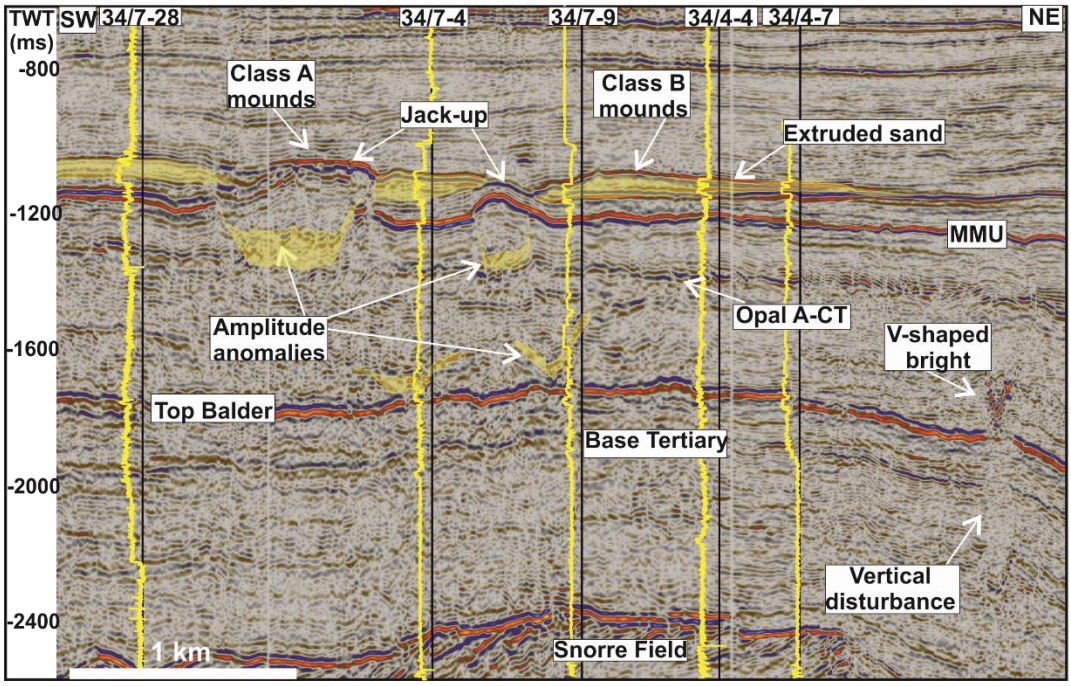
TWT (ms)
SW
34/7-28
34/7-4
34/7-9
34/4-4
34/4-7
NE
-800
-1200
-1600
-2000
-2400
Class A mounds
Jack-up
Class B mounds
Extruded sand
MMU
Opal A-CT
Amplitude anomalies
V-shaped bright
Top Balder
Base Tertiary
Vertical disturbance
1 km
Snorre Field

Fig. 10

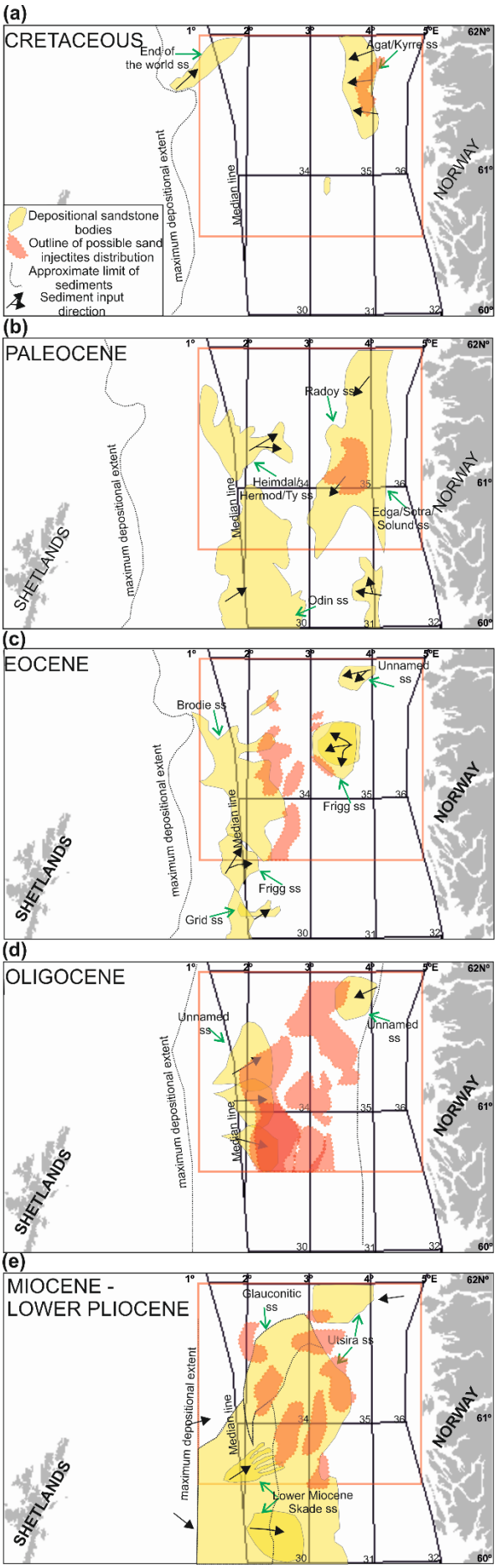
(a)
CRETACEOUS
End of the world ss
Agat/Kyrre ss
maximum depositional extent
Median line
NORWAY
Depositional sandstone bodies
Outline of possible sand injectites distribution
Approximate limit of sediments
Sediment input direction
(b)
PALEOCENE
Radoy ss
Heimdal/Hermod/Ty ss
Edga/Sotra/Solund ss
Odin ss
SHETLANDS
(c)
EOCENE
Unnamed ss
Brodie ss
Frigg ss
Grid ss
(d)
OLIGOCENE
(e)
MIOCENE - LOWER PLIOCENE
Glauconitic ss
Utsira ss
Lower Miocene Skade ss

Fig. 11

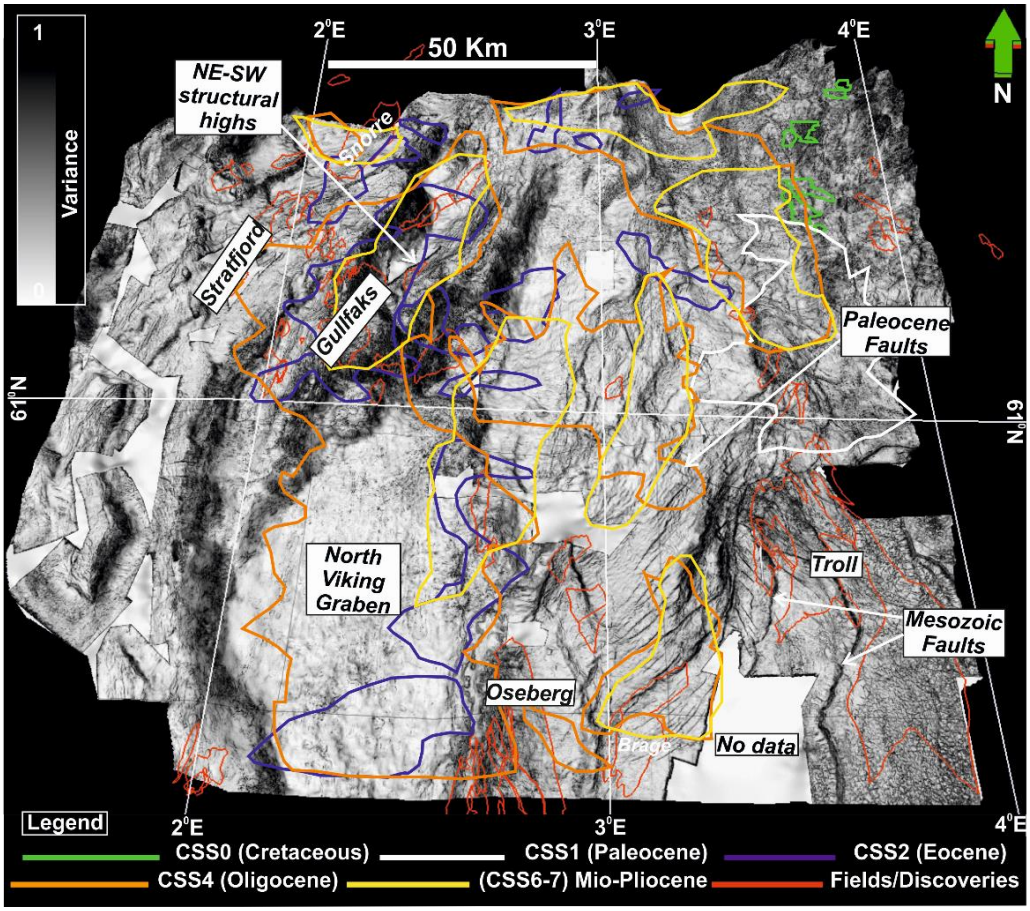
1
Variance
0
2°E
3°E
4°E
50 Km
N
NE-SW structural highs
Stord
Stratfjord
Gullfaks
Paleocene Faults
61°N
61°N
North Viking Graben
Troll
Mesozoic Faults
Oseberg
Brage
No data
Legend
CSS0 (Cretaceous)
CSS1 (Paleocene)
CSS2 (Eocene)
CSS4 (Oligocene)
(CSS6-7) Mio-Pliocene
Fields/Discoveries

Fig. 12

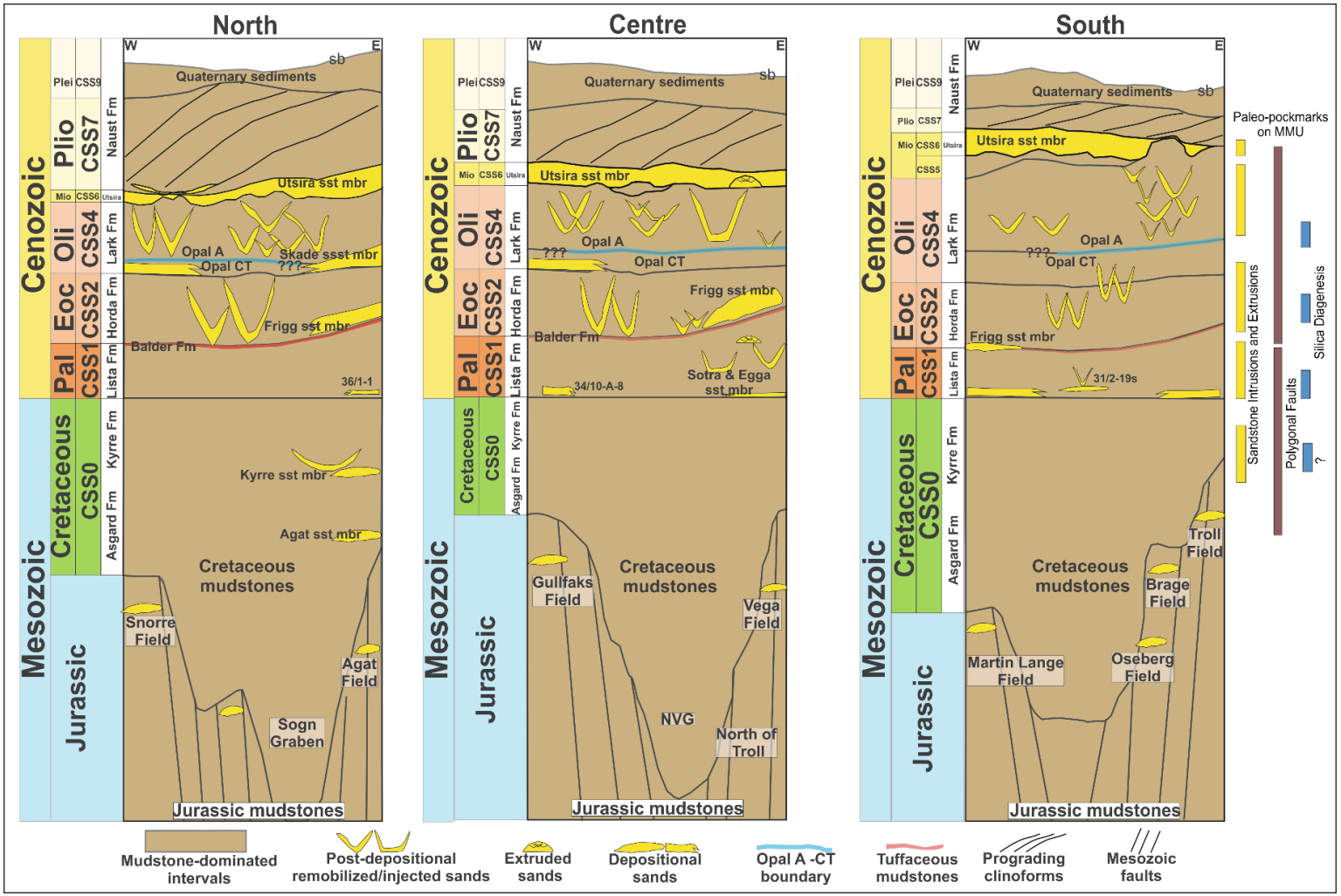
North
Centre
South
W
E
sb
Quaternary sediments
Utsira sst mbr
Opal A
Opal CT
???
Skade ssst mbr
Frigg sst mbr
Balder Fm
Sotra & Egga sst mbr
36/1-1
34/10-A-8
31/2-19s
Kyrre sst mbr
Agat sst mbr
Cretaceous mudstones
Snorre Field
Agat Field
Sogn Graben
Gullfaks Field
Vega Field
NVG
North of Troll
Brage Field
Troll Field
Martin Lange Field
Oseberg Field
Jurassic mudstones
Cenozoic
Mesozoic
Plei
Plio
Mio
Eoc
Oli
Pal
Cretaceous
Jurassic
CSS9
CSS7
CSS6
CSS5
CSS4
CSS2
CSS1
CSS0
Utsira
Naust Fm
Lark Fm
Horda Fm
Lista Fm
Kyrre Fm
Asgard Fm
Paleo-pockmarks on MMU
Sandstone Intrusions and Extrusions
Silica Diagenesis
Polygonal Faults
?
Mudstone-dominated intervals
Post-depositional remobilized/injected sands
Extruded sands
Depositional sands
Opal A -CT boundary
Tuffaceous mudstones
Prograding clinoforms
Mesozoic faults

Fig. 13

Intruded interval	Acoustic Impedance	Dip Angle	Dimensions (m)	Cross section/3D Geometry	Plan View Geometry	Overburden	Lithology	Timing	Injected/ Remobilized
CSS0 (Upper Cretaceous)	High-amplitude	1-20 (7°)	W: 150 - 1740 m; H: 7-90 m	Bedding concordant base and discordant margins	Channelized	Jack up, differential compaction	Sandstone confirmed from well	Upper cretaceous	Remobilized channels, extruded
CSS1 (Paleocene to Early Eocene)	High-amplitude, low- amplitude	17-32 (25°)	W: 440-1290m; H: 90-210 m	Same as CSS0, V-shaped geometries, mound	Isolated, oval-circular	Jack up, differential compaction	Sandstone confirmed from well	Middle Paleocene	Remobilized Channels, extruded
CSS2 (Early Eocene to Oligocene)	High-amplitude	14-37 (24°)	W: 490-1830m; H: 120-215m	V, U, W and saucer-shaped geometries	Isolated, circular	Jack up, sediment onlaps	Sandstone confirmed from well	Mid-Late Eocene	Injected remobilized
CSS3	No intrusions observed								
CSS4 (Oligocene to Miocene	High-amplitude, low- amplitude	12-35 (20°)	W: 500 – 1940m; H: 90-215m	V, U, W, saucers, ziz-zag, complex geometries	Isolated, oval, circular, complex	Jack up, sediment onlaps	Sandstone confirmed from well	Mid-Late Miocene	Injected, remobilized
CSS5	No intrusions observed								
CSS6	High-amplitude, low- amplitude	NA	Extensive	Mounded geometries	Circular, culmination	Sediment onlaps	Sandstone confirmed from well	Mid- Miocene to EarPliocene	Extruded
CSS7	High-amplitude, low- amplitude	NA	Extensive	Mounded geometries	Circular-elongated mounds	Sediment onlaps	Sandstone confirmed from well	Early Pliocene	Extruded
CSS8-9	No intrusions observed								